SUPPLEMENTARY INFORMATION

CoRa –A general approach for quantifying biological feedback control

Mariana Gómez-Schiavon[1], Hana El-Samad[1,2,3,4]

1 Department of Biochemistry and Biophysics, University of California, San Francisco, San Francisco, CA, USA.
2 Cell Design Initiative, University of California, San Francisco, CA, USA
3 Chan–Zuckerberg Biohub, San Francisco, CA, USA.
4 Cell Design Institute, San Francisco, CA, USA.

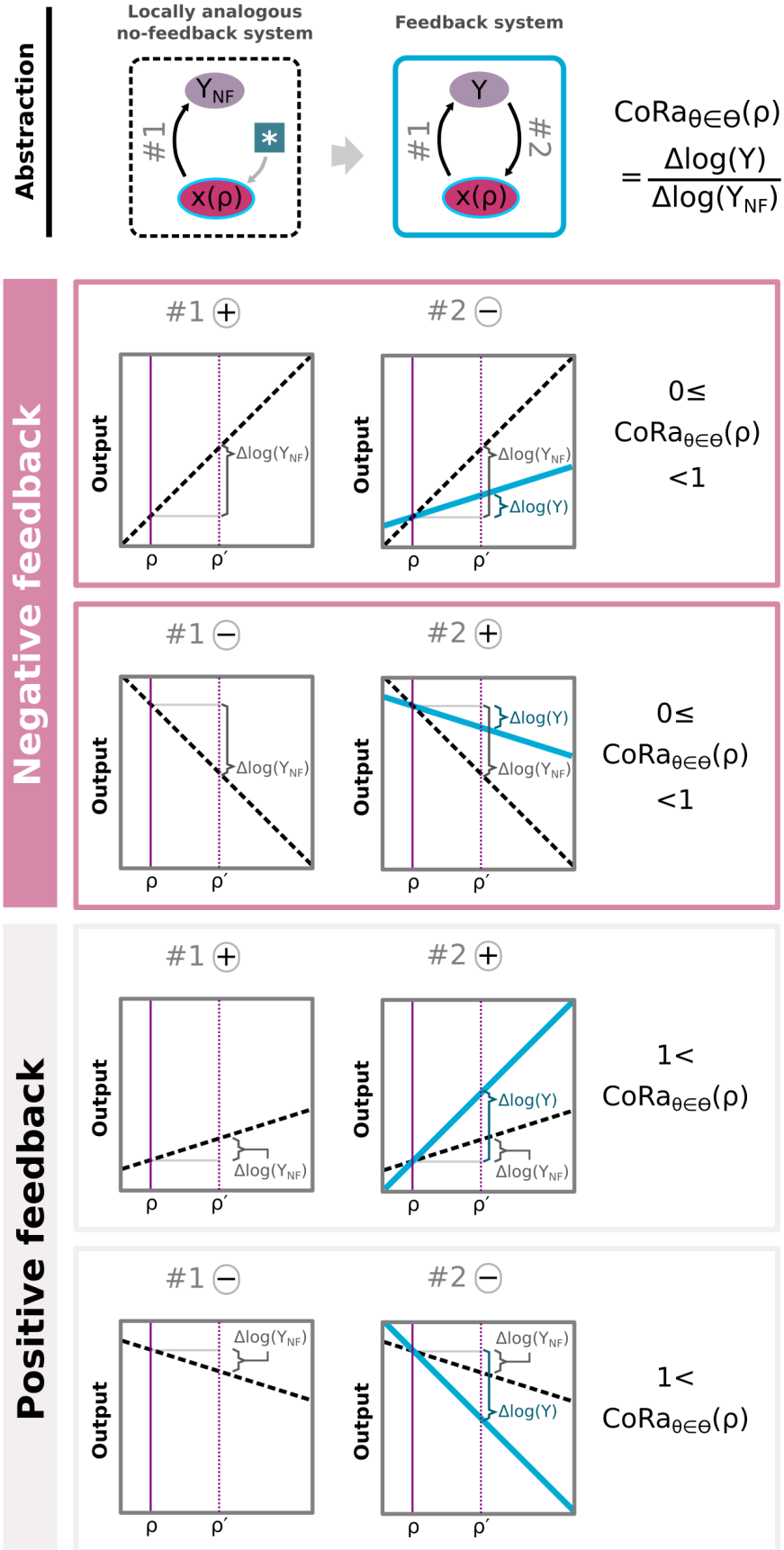

Figure S1. Feedback logic and CoRa values. We abstract the control system to a two-node network where one node represents the output to be controlled (Y), and the other the rest of the system including the dependency on the parameter ρ to be perturbed ($x(\rho)$). The locally analogous system can be represented as an equivalent network, with a third node ($*$) that represent the new input into the $x(\rho)$ node. The other link from $x(\rho)$ to the output (Y_{NF}; link #1) remains the same between the two networks. (Left column) The sign of link #1 can be determined by comparing the output before ($Y_{NF}|_\Theta = Y|_\Theta$) and after ($Y_{NF}|_{\Theta,\rho\to\rho'}$) the perturbation. For a positive perturbation, link #1 is positive (#1 (+)) if and only if $Y_{NF}|_{\Theta,\rho\to\rho'} > Y$, or negative (#1 (−)) if and only if $Y_{NF}|_{\Theta,\rho\to\rho'} < Y$. (Middle column) The sign of the feedback link from the output to the $x(\rho)$ node (link #2) can be determined by comparing the output after the perturbation in the feedback system ($Y|_{\Theta,\rho\to\rho'}$) and in the locally analogous system ($Y_{NF}|_{\Theta,\rho\to\rho'}$). It is positive (#2 (+)) if and only if $Y|_{\Theta,\rho\to\rho'} > Y_{NF}|_{\Theta,\rho\to\rho'}$, or negative (#2 (−)) if and only if $Y|_{\Theta,\rho\to\rho'} < Y_{NF}|_{\Theta,\rho\to\rho'}$. (Right column) Given the formula for CoRa, we can see that $\mathrm{CoRa}_{\theta\in\Theta}(\rho)$ is bound between 0 and 1 whenever we have a negative feedback, and bigger than 1 in the case of a positive feedback.

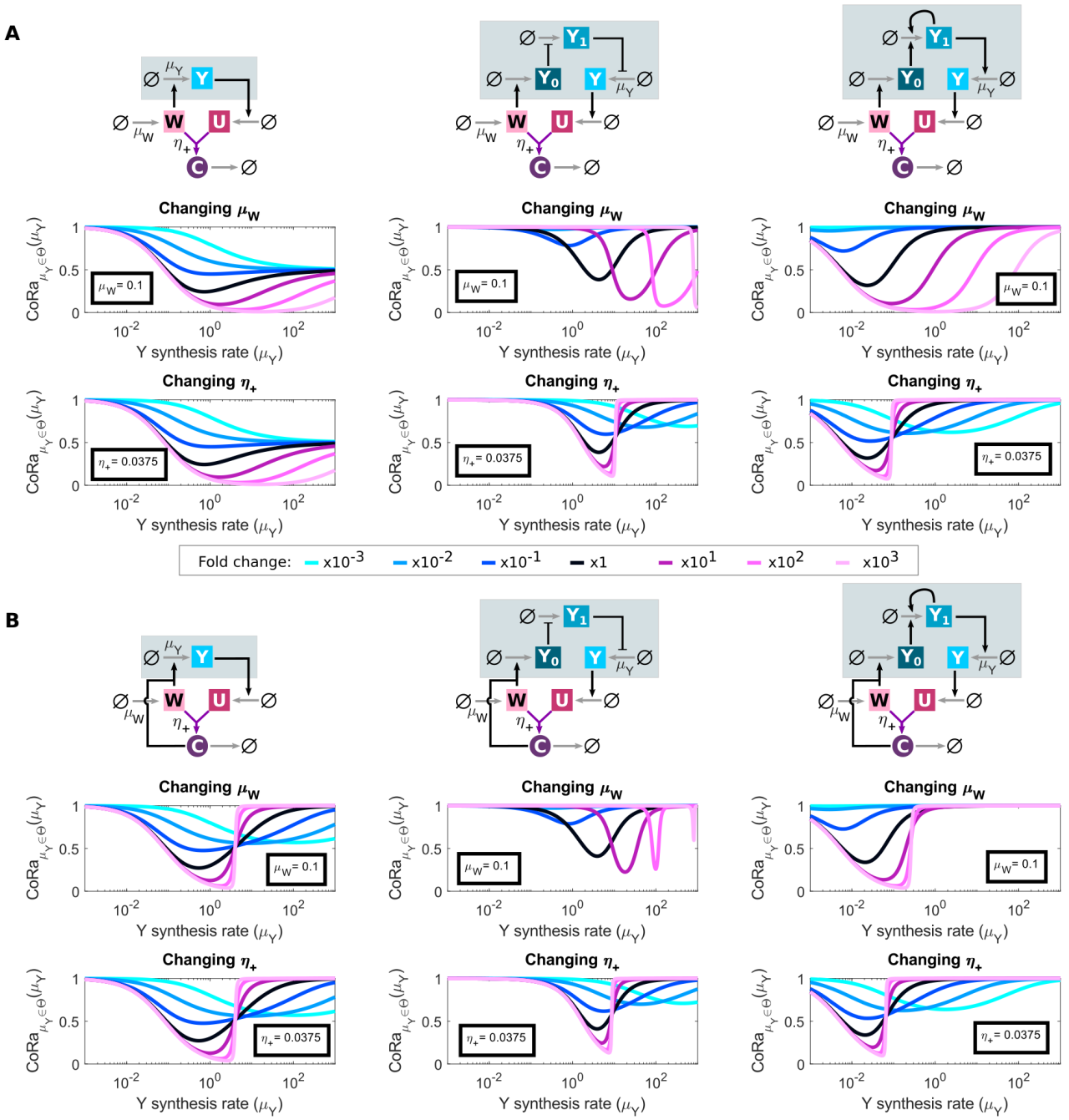

Figure S2. Antithetic feedback control performance depends on controlled subsystem. Three different subsystems (Eqs. 38-40) of increasing complexity (controlled subsystem highlighted in gray) controlled by the antithetic feedback control (ATF) can be compared using the CoRa function. **(A)** CoRa plots for modified ATF with inactive complex C (v1). First row shows a schematic controlled subsystem. $\text{CoRa}_{\mu_Y \in \Theta}(\mu_Y)$ is computed for 7 different values of a given parameter that is also varied in addition to μ_Y. The identity and nominal value of the varied parameter (either μ_W the W synthetic rate, or η_+ the $U : W$ binding rate) is indicated on every plot, and how it is varied is shown in between the two panels of the figure with appropriate color-coding information. **(B)** Same as **(A)** but modified ATF with active complex C (v2). See Section S4 for equations and Table S2 for parameter values.

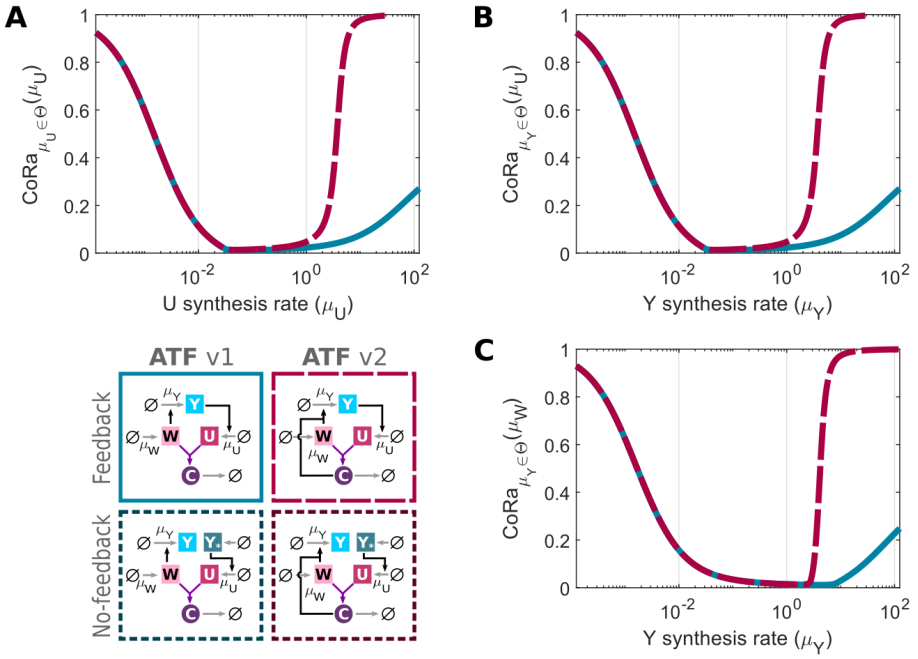

Figure S3. CoRa can be computed for perturbation of any parameter as a function of another parameters. Plots are shown for the two versions of the modified antithetic feedback (ATF) control. **(A)** CoRa plot as a function of U synthesis rate (μ_U) as μ_U itself is perturbed. **(B)** CoRa plot as a function of Y synthesis rate (μ_Y) as μ_U is perturbed. **(C)** CoRa plot as a function of Y synthesis rate (μ_Y) as W synthesis rate (μ_W) is perturbed. ATF v1, blue continuous lines; ATF v2, pink long-dash lines. See Section S4 for equations and Table S2 for parameter values.

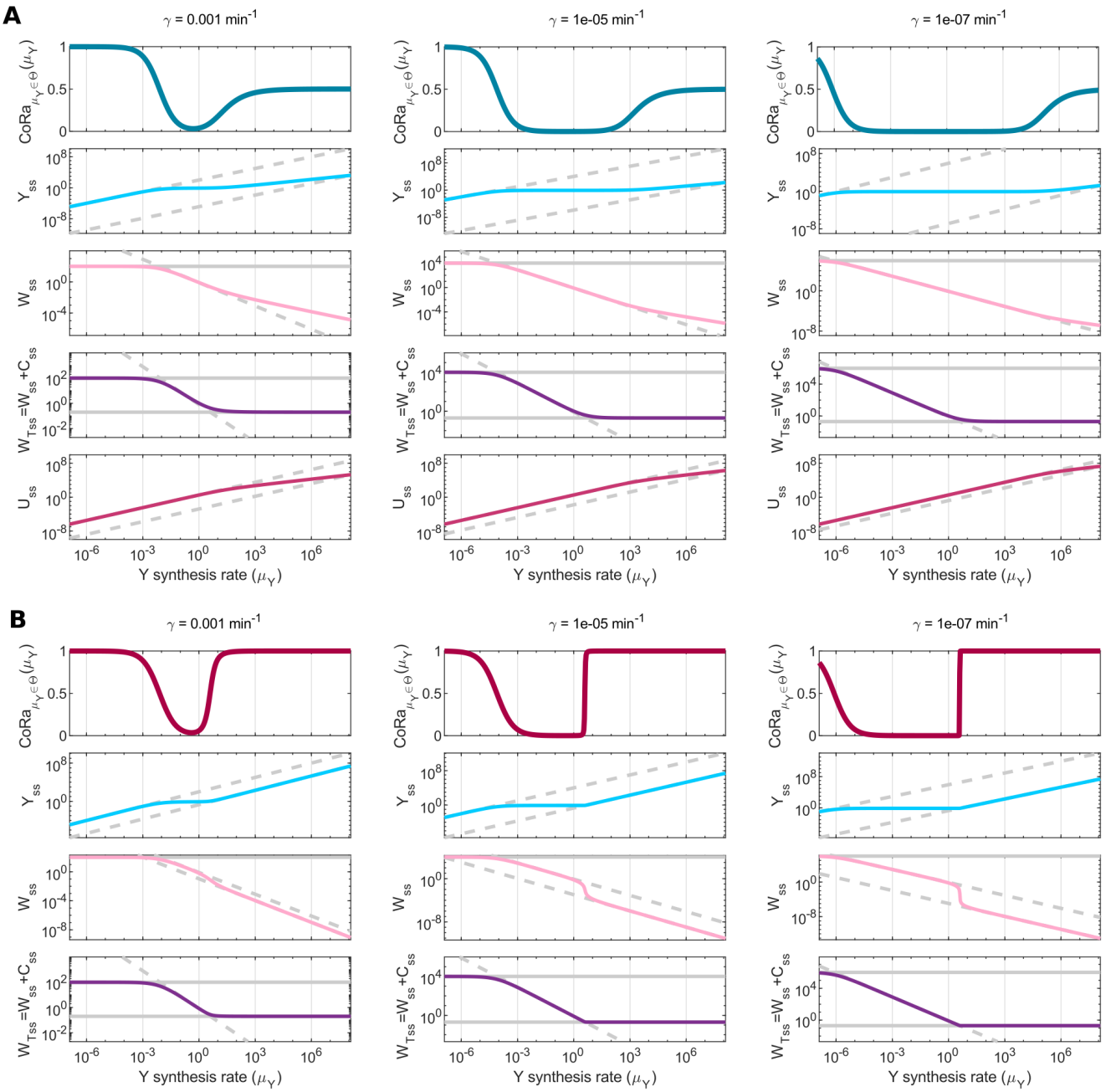

Figure S4. Effect of dilution on the modified antithetic feedback (ATF) control and system saturation. Effect of dilution (γ; see column titles) on the ATF control performance following perturbations to μ_Y, the synthesis rate of Y, as this parameter itself is varied, with either inactive (v1; **A**) or active (v2; **B**) complex C. **(A)** For ATF v1, as μ_Y decreases, $\text{CoRa}_{\mu_Y\in\Theta}(\mu_Y)$ increases. When W steady state concentration (W_{ss}) saturates approaching its limit value ($\frac{\mu_W}{\gamma+\gamma_W}$), $\text{CoRa}_{\mu_Y\in\Theta}(\mu_Y)$ approaches 1. On the other extreme, as μ_Y increases, $\text{CoRa}_{\mu_Y\in\Theta}(\mu_Y)$ increases. When total W at steady-state ($W_{T,ss} = W_{ss} + C_{ss}$) concentration saturates ($W_{T,ss} \to \frac{\mu_W}{\gamma+\gamma_W+\eta_-}$), U steady-state concentration (U_{ss}) cannot increase proportionally to μ_Y to allow free W_{ss} to decrease in the same proportion (given that in steady state, $W_{ss} = K_d\frac{C_{ss}}{U_{ss}}$; see Section S2.1.1). **(B)** For ATF v2, $\text{CoRa}_{\mu_Y\in\Theta}(\mu_Y)$ increases for both low and high μ_Y values as total W steady state concentration ($W_{T,ss} = W_{ss} + C_{ss}$) saturates, reaching its higher ($\frac{\mu_W}{\gamma+\gamma_W}$) and lower ($\frac{\mu_W}{\gamma+\gamma_W+\eta_-}$) limit values, respectively (see Section S2.1.2). In all plots, limits are shown as horizontal gray lines, and gray dashed lines increasing or decreasing proportionally to μ_Y are shown as reference. See Section S4 for equations and Table S2 for parameter values.

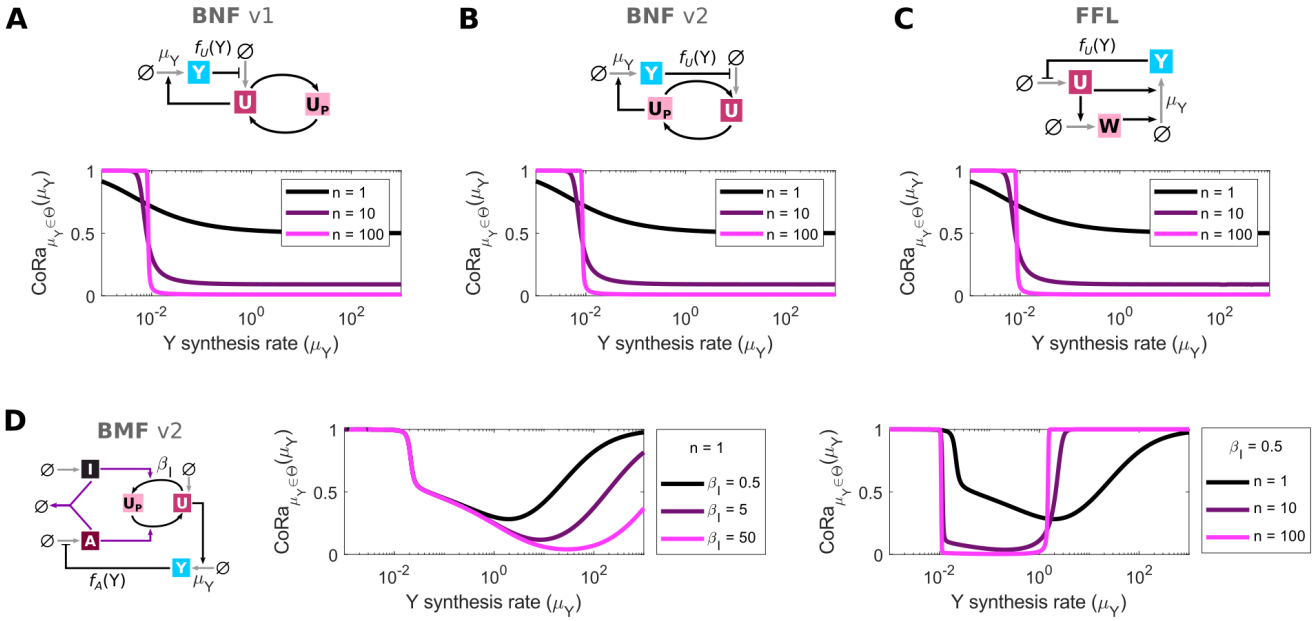

Figure S5. Negative auto-regulation affecting synthesis represented by Michaelis-Menten function limits control performance in multiple motifs, but is alleviated by ultrasensitivity. In this figure, the negative auto-regulation function is modeled as a negative Hill function, $f_{\square}(Y) = \mu_{\square}\frac{K_D^n}{Y^n+K_D^n}$, where $\mu_{\square}$ is the maximum synthesis rate, K_D is the EC_{50}, and n is the Hill coefficient. Four of the explored motifs in Fig. 3 include negative synthesis regulation ($f_{\square}(Y)$): **(A-B)** Buffering + Negative Feedback (BNF v1 & v2; Fig. 3G-H), **(C)** Feedback + Feedforward Loop (FFL; Fig. 3I), and **(D)** Brink Motif Feedback with repression of activator (BMF v2; Fig. 3K). For each motif, plots show CoRa function for perturbations to the Y synthesis rate (μ_Y) as the Hill coefficient n increases. (In all cases, the black line corresponds to the black line in Fig. 3). For **(D)** BMF v2, we also show how the CoRa function changes while increasing the inactivation rate β_I ($[nM^{-1}\,min^{-1}]$) from U to U_P, which is dependent on I. We corroborate that, as shown by Samaniego & Franco [8], the BMF motif displays high ultrasensitivity, and the ultrasensitivity increases as β_I increases. In all cases, higher ultrasensitivity (either by increasing the Hill coefficient n or β_I for BMFv2) results in improved control performance for some range of μ_Y values ($\text{CoRa}_{\mu_Y\in\Theta}(\mu_Y)$ approaching zero). See Section S4 for equations and Table S2 for parameter values.

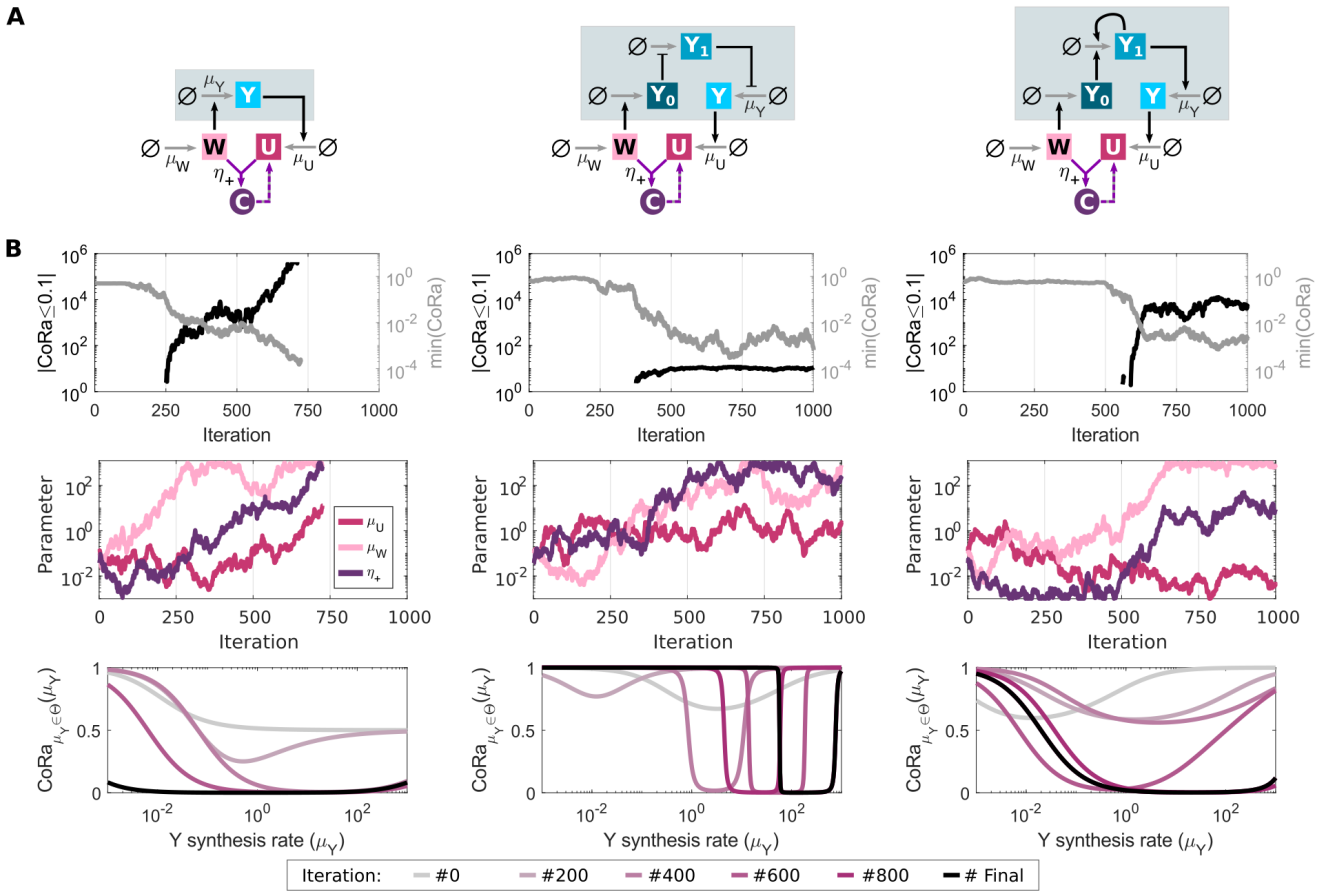

Figure S6. Optimizing a controller for different subsystems. (A) Diagrams for three different subsystems (Eqs. 38-40; gray boxes) that are controlled using the feedback by active degradation motif (FAD v1). **(B)** The feedback control parameters (U synthesis rate dependent on Y, μ_U; W constitutive synthesis rate, μ_W; and U, W binding rate, η_+) can be optimized for each subsystem to drive CoRa below a given threshold ($|\mathrm{CoRa}_{\mu_Y \in \Theta}(\mu_Y) \leq 0.1|$)for a large dynamic range in μ_Y, the synthesis rate of Y. The optimization stops after 1000 iterations or whenever $\mathrm{CoRa}_{\mu_Y \in \Theta}(\mu_Y) \leq 0.1$ for the whole range of μ_Y values considered; see *Section* S5.1 for algorithm details. Optimization traces ($\min(\mathrm{CoRa}_{\mu_Y \in \Theta}(\mu_Y))$, gray; $|\mathrm{CoRa}_{\mu_Y \in \Theta}(\mu_Y) \leq 0.1|$, black), as well as the associated parameter values ($\{\mu_U, \mu_W, \eta_+\}$), are shown for each system; the $\mathrm{CoRa}_{\mu_Y \in \Theta}(\mu_Y)$ curves for some iterations are also shown. See Section S4 for equations and Table S2 for parameter values.

Table S1. Used parameter values in main figures.

Fig. 2B	ATF v1 & v2 (Section S4.1)	$\gamma = 1 \times 10^{-4}\,min^{-1}$, $\gamma_U = 1 \times 10^{-4}\,min^{-1}$, $\gamma_W = 1 \times 10^{-4}\,min^{-1}$, $\mu_U = 0.125\,min^{-1}$, $\mu_W = 0.1\,nM\,min^{-1}$, $\eta_0 = 1 \times 10^{-4}\,min^{-1}$, $\eta_+ = 0.0375\,nM^{-1}\,min^{-1}$, $\eta_- = 0.5\,min^{-1}$, $\gamma_Y = 1\,min^{-1}$
Fig. 2C	ATF v1 & v2 (Section S4.1)	$\gamma = 1 \times 10^{-4}\,min^{-1}$, $\gamma_U = 1 \times 10^{-4}\,min^{-1}$, $\gamma_W = 1 \times 10^{-4}\,min^{-1}$, $\mu_U = 0.125\,min^{-1}$, $\mu_W = 0.1\,nM\,min^{-1}$, $\eta_0 = 1 \times 10^{-4}\,min^{-1}$, $\eta_+ = 0.0375\,nM^{-1}\,min^{-1}$, $\mu_Y = 0.125\,min^{-1}$, $\gamma_Y = 1\,min^{-1}$
Fig. 2D	ATF v1 & v2 (Section S4.1)	$\gamma = 1 \times 10^{-4}\,min^{-1}$, $\gamma_U = 1 \times 10^{-4}\,min^{-1}$, $\gamma_W = 1 \times 10^{-4}\,min^{-1}$, $\mu_U = 0.125\,min^{-1}$, $\mu_W = 0.1\,nM\,min^{-1}$, $\eta_0 = 1 \times 10^{-4}\,min^{-1}$, $\eta_+ = 0.0375\,nM^{-1}\,min^{-1}$, $\eta_- = 0.5\,min^{-1}$, $\gamma_Y = 1\,min^{-1}$, $\mu_Y^{(i)} = \{0.3863, 3.9, 125\}\,min^{-1}$
Fig. 3A	ATF v1 (Section S4.1)	$\gamma = 0.01\,min^{-1}$, $\gamma_U = 1 \times 10^{-4}\,min^{-1}$, $\gamma_W = 1 \times 10^{-4}\,min^{-1}$, $\mu_U = 0.125\,min^{-1}$, $\eta_0 = 1 \times 10^{-4}\,min^{-1}$, $\eta_+ = 0.0375\,nM^{-1}\,min^{-1}$, $\eta_- = 0.5\,min^{-1}$, $\gamma_Y = 0.1\,min^{-1}$, $\mu_W = 1.015\,nM\,min^{-1}$ (black line; $Y \approx 10\,nM$ for $\mu_Y = 1\,min^{-1}$).
Fig. 3B	FAD v1 (Section S4.2)	$\gamma = 0.01\,min^{-1}$, $\gamma_U = 0.05\,min^{-1}$, $\gamma_W = 1 \times 10^{-4}\,min^{-1}$, $\mu_U = 0.125\,min^{-1}$, $\eta_0 = 1 \times 10^{-4}\,min^{-1}$, $\eta_+ = 0.0375\,nM^{-1}\,min^{-1}$, $\eta_- = 0.5\,min^{-1}$, $\gamma_Y = 0.1\,min^{-1}$, $\mu_W = 0.74\,nM\,min^{-1}$ (black line; $Y \approx 10\,nM$ for $\mu_Y = 1\,min^{-1}$).
Fig. 3C	FDP v1 (Section S4.3)	$\gamma = 0.01\,min^{-1}$, $\gamma_U = 0.05\,min^{-1}$, $\gamma_W = 1 \times 10^{-4}\,min^{-1}$, $\mu_U = 0.125\,min^{-1}$, $\eta_0 = 1 \times 10^{-4}\,min^{-1}$, $\eta_+ = 0.0375\,nM^{-1}\,min^{-1}$, $\eta_- = 0.5\,min^{-1}$, $K_D = 0.02\,nM$, $\gamma_Y = 0.1\,min^{-1}$, $\mu_W = 0.7545\,nM\,min^{-1}$ (black line; $Y \approx 10\,nM$ for $\mu_Y = 1\,min^{-1}$).
Fig. 3D	ATF v2 (Section S4.1)	$\gamma = 0.01\,min^{-1}$, $\gamma_U = 1 \times 10^{-4}\,min^{-1}$, $\gamma_W = 1 \times 10^{-4}\,min^{-1}$, $\mu_U = 0.125\,min^{-1}$, $\eta_0 = 1 \times 10^{-4}\,min^{-1}$, $\eta_+ = 0.0375\,nM^{-1}\,min^{-1}$, $\eta_- = 0.5\,min^{-1}$, $\gamma_Y = 0.1\,min^{-1}$, $\mu_W = 0.478\,nM\,min^{-1}$ (black line; $Y \approx 10\,nM$ for $\mu_Y = 1\,min^{-1}$).
Fig. 3E	FAD v2 (Section S4.2)	$\gamma = 0.01\,min^{-1}$, $\gamma_U = 0.05\,min^{-1}$, $\gamma_W = 1 \times 10^{-4}\,min^{-1}$, $\mu_U = 0.125\,min^{-1}$, $\eta_0 = 1 \times 10^{-4}\,min^{-1}$, $\eta_+ = 0.0375\,nM^{-1}\,min^{-1}$, $\eta_- = 0.5\,min^{-1}$, $\gamma_Y = 0.1\,min^{-1}$, $\mu_W = 0.327\,nM\,min^{-1}$ (black line; $Y \approx 10\,nM$ for $\mu_Y = 1\,min^{-1}$).
Fig. 3F	FDP v2 (Section S4.3)	$\gamma = 0.01\,min^{-1}$, $\gamma_U = 0.05\,min^{-1}$, $\gamma_W = 1 \times 10^{-4}\,min^{-1}$, $\mu_U = 0.125\,min^{-1}$, $\eta_0 = 1 \times 10^{-4}\,min^{-1}$, $\eta_+ = 0.0375\,nM^{-1}\,min^{-1}$, $\eta_- = 0.5\,min^{-1}$, $K_D = 0.02\,nM$, $\gamma_Y = 0.1\,min^{-1}$, $\mu_W = 0.333\,nM\,min^{-1}$ (black line; $Y \approx 10\,nM$ for $\mu_Y = 1\,min^{-1}$).
Fig. 3G	BNF v1 (Section S4.4)	$\gamma = 0.01\,min^{-1}$, $\gamma_U = 1 \times 10^{-4}\,min^{-1}$, $\mu_U = 2\,min^{-1}$, $K_D = 1\,nM$, $\gamma_Y = 0.1\,min^{-1}$, $\beta = 0.1565\,min^{-1}$, $\beta_P = 1 \times 10^{-4}\,min^{-1}$ (black line; $Y \approx 10\,nM$ for $\mu_Y = 1\,min^{-1}$).
Fig. 3H	BNF v2 (Section S4.4)	$\gamma = 0.01\,min^{-1}$, $\gamma_U = 1 \times 10^{-4}\,min^{-1}$, $\mu_U = 2\,min^{-1}$, $K_D = 1\,nM$, $\gamma_Y = 0.1\,min^{-1}$, $\beta = 0.0108\,min^{-1}$, $\beta_P = 0.1565\,min^{-1}$ (black line; $Y \approx 10\,nM$ for $\mu_Y = 1\,min^{-1}$).
Fig. 3I	FFL v1 (Section S4.5)	$\gamma = 0.01\,min^{-1}$, $\gamma_U = 0.01\,min^{-1}$, $\gamma_W = 0.01\,min^{-1}$, $\mu_W = 0.125\,min^{-1}$, $K_D = 1\,nM$, $\gamma_Y = 0.1\,min^{-1}$, and $\mu_U = 0.0334\,min^{-1}$ (black line; $Y \approx 10\,nM$ for $\mu_Y = 1\,min^{-1}$).
Fig. 3J	BMF v1 (Section S4.6)	$\gamma = 0.01\,min^{-1}$, $\mu_U = 0.1\,nM\,min^{-1}$, $\eta_0 = 1 \times 10^{-4}\,min^{-1}$, $\eta_+ = 0.05\,nM^{-1}\,min^{-1}$, $\beta_A = 0.5\,nM^{-1}\,min^{-1}$, $\beta_I = 0.5\,nM^{-1}\,min^{-1}$, $\gamma_Y = 0.1\,min^{-1}$, $\mu_A = 0.0338\,nM\,min^{-1}$, $\mu_I = 0.0125\,min^{-1}$ (black line; $Y \approx 10\,nM$ for $\mu_Y = 1\,min^{-1}$).
Fig. 3K	BMF v2 (Section S4.6)	$\gamma = 0.01\,min^{-1}$, $\mu_U = 0.1\,nM\,min^{-1}$, $\eta_0 = 1 \times 10^{-4}\,min^{-1}$, $\eta_+ = 0.05\,nM^{-1}\,min^{-1}$, $\beta_A = 0.5\,nM^{-1}\,min^{-1}$, $\beta_I = 0.5\,nM^{-1}\,min^{-1}$, $\gamma_Y = 0.1\,min^{-1}$, $\mu_A = 0.372\,nM\,min^{-1}$, $K_D = 1\,nM$, $\mu_I = 0.125\,nM\,min^{-1}$ (black line; $Y \approx 10\,nM$ for $\mu_Y = 1\,min^{-1}$).

Table S2. Used parameter values in supplementary figures.

Fig. S2A	ATF v1 (Section S4.1 & Section S2.2)	$\gamma = 0.01\,min^{-1}$, $\gamma_U = \gamma_W = 1 \times 10^{-4}\,min^{-1}$, $\mu_U = 0.125\,min^{-1}$, $\mu_W = 0.1\,nM\,min^{-1}$, $\eta_0 = 1 \times 10^{-4}\,min^{-1}$, $\eta_+ = 0.0375\,nM^{-1}\,min^{-1}$, $\eta_- = 0.5\,min^{-1}$, $\gamma_Y = 1\,min^{-1}$; and specifically for the double-negative subsystem: $K_D = 1\,nM$, $\mu_0 = 1.25\,min^{-1}$, $\mu_1 = 12.5\,nM\,min^{-1}$, $K_1 = 1\,nM$, and for the subsystem with positive feedback: $\mu_0 = 1.25\,min^{-1}$, $\mu_1 = 12.5\,nM\,min^{-1}$, $\mu_P = 10\,nM\,min^{-1}$, $K_P = 1\,nM$ (black lines).
Fig. S2B	ATF v2 (Section S4.1 & Section S2.2)	$\gamma = 0.01\,min^{-1}$, $\gamma_U = \gamma_W = 1 \times 10^{-4}\,min^{-1}$, $\mu_U = 0.125\,min^{-1}$, $\mu_W = 0.1\,nM\,min^{-1}$, $\eta_0 = 1 \times 10^{-4}\,min^{-1}$, $\eta_+ = 0.0375\,nM^{-1}\,min^{-1}$, $\eta_- = 0.5\,min^{-1}$, $\gamma_Y = 1\,min^{-1}$; and specifically for the double-negative subsystem: $K_D = 1\,nM$, $\mu_0 = 1.25\,min^{-1}$, $\mu_1 = 12.5\,nM\,min^{-1}$, $K_1 = 1\,nM$, and for the subsystem with positive feedback: $\mu_0 = 1.25\,min^{-1}$, $\mu_1 = 12.5\,nM\,min^{-1}$, $\mu_P = 10\,nM\,min^{-1}$, $K_P = 1\,nM$ (black lines).
Fig. S3	ATF v1 & v2 (Section S4.1)	$\gamma = 1 \times 10^{-4}\,min^{-1}$, $\gamma_U = 1 \times 10^{-4}\,min^{-1}$, $\gamma_W = 1 \times 10^{-4}\,min^{-1}$, $\mu_W = 0.1\,nM\,min^{-1}$, $\eta_0 = 1 \times 10^{-4}\,min^{-1}$, $\eta_+ = 0.0375\,nM^{-1}\,min^{-1}$, $\eta_- = 0.5\,min^{-1}$, $\gamma_Y = 1\,min^{-1}$, and $\mu_Y = 0.125\,min^{-1}$, $\mu_U = 0.125\,min^{-1}$, unless explicitly varied.
Fig. S4A	ATF v1 (Section S4.1)	$\gamma_U = \gamma_W = 0$, $\mu_U = 0.125\,min^{-1}$, $\mu_W = 0.1\,nM\,min^{-1}$, $\eta_0 = 1 \times 10^{-4}\,min^{-1}$, $\eta_+ = 0.0375\,nM^{-1}\,min^{-1}$, $\eta_- = 0.5\,min^{-1}$, $\gamma_Y = 1\,min^{-1}$, $\gamma = \{0.001, 1 \times 10^{-5}, 1 \times 10^{-7}\}\,min^{-1}$
Fig. S4B	ATF v2 (Section S4.1)	$\gamma_U = \gamma_W = 0$, $\mu_U = 0.125\,min^{-1}$, $\mu_W = 0.1\,nM\,min^{-1}$, $\eta_0 = 1 \times 10^{-4}\,min^{-1}$, $\eta_+ = 0.0375\,nM^{-1}\,min^{-1}$, $\eta_- = 0.5\,min^{-1}$, $\gamma_Y = 1\,min^{-1}$, $\gamma = \{0.001, 1 \times 10^{-5}, 1 \times 10^{-7}\}\,min^{-1}$
Fig. S5A	BNF v1 (Section S4.4)	$\gamma = 0.01\,min^{-1}$, $\gamma_U = 1 \times 10^{-4}\,min^{-1}$, $\mu_U = 2\,min^{-1}$, $K_D = 1\,nM$, $\gamma_Y = 0.1\,min^{-1}$, $\beta = 0.1565\,min^{-1}$, $\beta_P = 1 \times 10^{-4}\,min^{-1}$, $n = \{1, 10, 100\}$.
Fig. S5B	BNF v2 (Section S4.4)	$\gamma = 0.01\,min^{-1}$, $\gamma_U = 1 \times 10^{-4}\,min^{-1}$, $\mu_U = 2\,min^{-1}$, $K_D = 1\,nM$, $\gamma_Y = 0.1\,min^{-1}$, $\beta = 0.0108\,min^{-1}$, $\beta_P = 0.1565\,min^{-1}$, $n = \{1, 10, 100\}$.
Fig. S5C	FFL v1 (Section S4.5)	$\gamma = 0.01\,min^{-1}$, $\gamma_U = 0.01\,min^{-1}$, $\gamma_W = 0.01\,min^{-1}$, $\mu_W = 0.125\,min^{-1}$, $K_D = 1\,nM$, $\gamma_Y = 0.1\,min^{-1}$, and $\mu_U = 0.0334\,min^{-1}$, $n = \{1, 10, 100\}$.
Fig. S5D	BMF v2 (Section S4.6)	$\gamma = 0.01\,min^{-1}$, $\mu_U = 0.1\,nM\,min^{-1}$, $\eta_0 = 1 \times 10^{-4}\,min^{-1}$, $\eta_+ = 0.05\,nM^{-1}\,min^{-1}$, $\beta_A = 0.5\,nM^{-1}\,min^{-1}$, $\gamma_Y = 0.1\,min^{-1}$, $\mu_A = 0.372\,nM\,min^{-1}$, $K_D = 1\,nM$, $\mu_I = 0.125\,nM\,min^{-1}$, $n = \{1, 10, 100\}$, $\beta_I = \{0.5, 5, 50\}\,nM^{-1}\,min^{-1}$.
Fig. S6B	FAD v1 (Section S4.2 & Section S2.2)	$\gamma = 0.01\,min^{-1}$, $\gamma_U = 0.05\,min^{-1}$, $\gamma_W = 1 \times 10^{-4}\,min^{-1}$, $\eta_0 = 1 \times 10^{-4}\,min^{-1}$, $\eta_- = 0.5\,min^{-1}$, $\gamma_Y = 1\,min^{-1}$; and specifically for the double-negative subsystem: $K_D = 1\,nM$, $\mu_0 = 1.25\,min^{-1}$, $\mu_1 = 12.5\,nM\,min^{-1}$, $K_1 = 1\,nM$, and for the subsystem with positive feedback: $\mu_0 = 1.25\,min^{-1}$, $\mu_1 = 12.5\,nM\,min^{-1}$, $\mu_P = 10\,nM\,min^{-1}$, $K_P = 1\,nM$; initial parameter values: $\mu_U = 0.125\,min^{-1}$, $\mu_W = 0.1\,nM\,min^{-1}$, $\eta_+ = 0.0375\,nM^{-1}\,min^{-1}$.

Note: Across this document, capital letters (e.g. X) represent both the species and its concentration; the sub-index X_{ss} refers to the steady state value; and lower-case Greek letters represent parameters, which by default are non-negative real numbers.

S1 CoRa approach

CoRa –or ***Co**ntrol **Ra**tio*– aims to quantify the effect of feedback control on a system's ability to reject a step perturbation, while considering the effect and constraints of the individual biochemical events. This is done by directly comparing the feedback system of interest to a locally analogous system without feedback under the formalism of *mathematically controlled comparisons* [1]. Each locally analogous system has exactly the same biochemical reactions and parameters as the original feedback system (i.e. *internal equivalence*), with the exception of the feedback input from the controlled subsystem. For each specific parameter set Θ (i.e. the value of all parameters describing the system of interest), the feedback input is substituted by an equivalent constant input calibrated such that the steady-state of all common species between the two systems are identical before a perturbation is applied (i.e. *external equivalence*). This equivalence allows for a direct comparison of the output change of both systems following a specific step perturbation (e.g. step change in a parameter value), while accounting for the influence of the nonlinearity, saturation, and other intrinsic particularities of the system, and guarantying that any differential response of these two analogous systems represents an *inherent functional difference* associated with the feedback control. The perturbation considered must not affect the constant input of the locally analogous system, as otherwise the differential output response can no longer be uniquely associated with the feedback control.

Let $Y_{ss}|_\Theta$ denote the steady-state value of the system with feedback for a parameter set Θ, and $Y_{ss,NF}|_\Theta$ denote the steady-state value of the locally analogous system without feedback. Let's also consider a a small step perturbation of a specific parameter $\rho \in \Theta$ ($\rho \to \rho'$). Following this perturbation, $Y_{ss}|_{\Theta,\rho\to\rho'}$ and $Y_{ss,NF}|_{\Theta,\rho\to\rho'}$ denote that new steady-states of the feedback system and locally analogous system without feedback,respectively.

CoRa is then defined as:

$$\begin{aligned}
\mathrm{CoRa}_{\theta\in\Theta}(\rho) &= \frac{\Delta\log(\mathrm{Y_{ss}})|_{\Theta,\rho\to\rho'}}{\Delta\log(\mathrm{Y_{ss,NF}})|_{\Theta,\rho\to\rho'}} \\
&= \frac{\log(Y_{ss}|_{\Theta,\rho\to\rho'}) - \log(Y_{ss}|_\Theta)}{\log(Y_{ss,NF}|_{\Theta,\rho\to\rho'}) - \log(Y_{ss,NF}|_\Theta)} \\
&= \frac{\log\left(\frac{Y_{ss}|_{\Theta,\rho\to\rho'}}{Y_{ss}|_\Theta}\right)}{\log\left(\frac{Y_{ss,NF}|_{\Theta,\rho\to\rho'}}{Y_{ss,NF}|_\Theta}\right)}
\end{aligned} \tag{1}$$

Note that by construction the output of the feedback system and the locally analogous system without feedback are identical before a perturbation, i.e. $Y_{ss}|_\Theta = Y_{ss,NF}|_\Theta$.

Assuming that $\Delta\rho = \rho' - \rho$ is small enough, the output of the feedback system and the locally analogous system without feedback can be expressed as linear functions of $\Delta\rho$. The corresponding CoRa function can then be written as:

$$\begin{aligned}
\mathrm{CoRa}_{\theta\in\Theta}(\rho) &= \frac{\log(Y_{ss}(\rho+\Delta\rho)) - \log(Y_{ss}(\rho))}{\log(Y_{ss,NF}(\rho+\Delta\rho)) - \log(Y_{ss,NF}(\rho))} \\
&\approx \frac{\log(Y_{ss}(\rho)) + \Delta\rho\frac{d}{d\rho}\log(Y_{ss})|_\rho - \log(Y_{ss}(\rho))}{\log(Y_{ss,NF}(\rho)) + \Delta\rho\frac{d}{d\rho}\log(Y_{ss,NF})|_\rho - \log(Y_{ss,NF}(\rho))} \\
&\approx \frac{\frac{d}{d\rho}\log(Y_{ss})|_\rho}{\frac{d}{d\rho}\log(Y_{ss,NF})|_\rho}
\end{aligned} \tag{2}$$

Eq. 2 shows that in this regime, CoRa value is approximately independent of the perturbation size $\Delta\rho$. In all the analyses presented on this paper, we used $\rho' = 1.05\rho$. We corroborated that this perturbation size was small enough to reach the linear regime by confirming that identical results were obtained with $\rho' = 1.01\rho$. Nevertheless, with the smaller perturbation size ($\rho' = 1.01\rho$), noise in the numerical solutions was observed for some cases. In general, like

for any linearization exercise, the acceptable perturbation size for numerical solutions needs to be evaluated for the specific system and conditions of interest.

The value of $\mathrm{CoRa}_{\theta\in\Theta}(\rho)$ can be easily related to the logic of the feedback (Fig. S1). If $\mathrm{CoRa}_{\theta\in\Theta}(\rho) \in [0,1)$, the presence of the feedback reduces the effect of the perturbation compared to the locally analogous system without feedback, i.e. the system has an active negative feedback: either $0 \leq \Delta\log(Y_{ss})|_{\Theta,\rho\to\rho'} < \Delta\log(Y_{ss,NF})|_{\Theta,\rho\to\rho'}$ or $0 \geq \Delta\log(Y_{ss})|_{\Theta,\rho\to\rho'} > \Delta\log(Y_{ss,NF})|_{\Theta,\rho\to\rho'}$. On the other hand, if $\mathrm{CoRa}_{\theta\in\Theta}(\rho) > 1$, the presence of the feedback amplifies the effect of the perturbation compared to the locally analogous system without feedback, i.e. the system has an active positive feedback: either $\Delta\log(Y_{ss})|_{\Theta,\rho\to\rho'} > \Delta\log(Y_{ss,NF})|_{\Theta,\rho\to\rho'} > 0$ or $\Delta\log(Y_{ss})|_{\Theta,\rho\to\rho'} < \Delta\log(Y_{ss,NF})|_{\Theta,\rho\to\rho'} < 0$. Finally, if $\mathrm{CoRa}_{\theta\in\Theta}(\rho) = 1$, the feedback is effectively inactive. As the goal of CoRa is to quantify feedback control, which by definition requires a corrective (negative) feedback regulation, $\mathrm{CoRa}_{\theta\in\Theta}(\rho)$ is bounded between 0 and 1 for the cases of interest. More specifically, $\mathrm{CoRa}_{\theta\in\Theta}(\rho) = 0$ only if the system displays perfect control ($Y_{ss}|_{\Theta,\rho\to\rho'} = Y_{ss}|_{\Theta}$), and $\mathrm{CoRa}_{\theta\in\Theta}(\rho)$ value increases as the control effect decreases up until $\mathrm{CoRa}_{\theta\in\Theta}(\rho) = 1$, when the feedback contribution is effectively zero (i.e. the system response to the perturbation is exactly the same that the one of the system without feedback).

S2 Analysis of a modified antithetic feedback control strategy using CoRa

We consider a modified *antithetic feedback motif* (ATF; based on Briat *et al.* [2]) with a simple controlled subsystem consisting of a single molecule Y. The ATF motif consists of two molecules U and W that bind to each other forming a transitory complex C. C is then degraded leading to the disappearance of both U and W. Y is produced at a rate that depends on the concentration of W, while U synthesis is induced by Y. The equations of the full system with feedback are then given by:

$$\frac{d}{dt}U = \mu_U Y - (\gamma+\gamma_U)U - \eta_+ UW + (\eta_0+\gamma_W)C \tag{3}$$

$$\frac{d}{dt}W = \mu_W - (\gamma+\gamma_W)W - \eta_+ UW + (\eta_0+\gamma_U)C \tag{4}$$

$$\frac{d}{dt}C = \eta_+ UW - (\gamma+\eta_0+\eta_-+\gamma_U+\gamma_W)C \tag{5}$$

For Y dynamics, two alternative scenarios can be easily foreseen: W can be either inactivated as a transcription factor once it binds U (ATF v1; Fig. 2A,3A),

$$\frac{d}{dt}Y = \mu_Y W - (\gamma+\gamma_Y)Y \tag{6}$$

or W retains its transcription factor activity until degraded (ATF v2; Fig. 2A,3D),

$$\frac{d}{dt}Y = \mu_Y (W+C) - (\gamma+\gamma_Y)Y \tag{7}$$

Here all species are subject to loss by dilution (γ), in addition of their own individual degradation rates ($\gamma_\square$), $\mu_\square$ represents the synthesis rate for each molecule (either constitutive, μ_W, or dependent of a transcription factor, μ_U and μ_Y), and η_- is the co-degradation rate of U, W in the complex form C; η_+ is the binding rate of U and W (forming the complex C); and η_0 is the spontaneous unbinding rate of these two molecules (dissociating the complex C).

Choosing Y as the system's output, the corresponding locally analogous system without feedback maintains the same ODE equations (Eqs. 4-5, and either Eq. 6 or Eq. 7), with the exception of $\frac{dU}{dt}$,

$$\frac{d}{dt}U = \mu_U Y_* - (\gamma+\gamma_U)U - \eta_+ UW + (\eta_0+\gamma_W)C \tag{8}$$

where U synthesis rate now depends on a new molecule Y_* with dynamics

$$\frac{d}{dt}Y_* = \mu_{Y_*} - (\gamma+\gamma_{Y_*})Y_* \tag{9}$$

such that Y_* is constitutively expressed with synthesis μ_{Y*}. If $\gamma_{Y*} = \gamma_Y$, then the steady state output of the locally analogous system without feedback $Y_{ss,NF}$ is equal to the steady state output of the feedback system Y_{ss} if either $\mu_{Y*} = \mu_Y W_{ss}$ or $\mu_{Y*} = \mu_Y(W_{ss} + C_{ss})$, depending on the feedback system being considered (ATF v1 or ATF v2).

In this case, since Y_* in the locally analogous system without feedback does not depend on any other molecule in the system, its concentration will remain constant after any type of perturbation. As mentioned above, this is an important requirement for the mathematically controlled comparison: if a perturbation also affects Y_* value (e.g. experimental perturbations on dilution, γ), the feedback system and the locally analogous system differ in more than just the feedback information (Fig. S1D), and the CoRa value cannot be interpreted as simply the feedback contribution.

As described by Briat *et al.* [2], assuming there is no dilution ($\gamma = 0$) as well as no individual degradation of U and W (i.e. independent of the complex formation C; $\gamma_U, \gamma_W = 0$), this system (Eqs. 4-5) is expected to display perfect step disturbance rejection (integral control or perfect adaptation):

$$\begin{aligned} \frac{d}{dt}U &= \mu_U Y - \eta_+ UW + \eta_0 C \\ \frac{d}{dt}W &= \mu_W - \eta_+ UW + \eta_0 C \\ \text{then } \frac{d}{dt}(U - W) &= \mu_U Y - \mu_W \\ \text{and if } \frac{d}{dt}U_{ss} = \frac{d}{dt}W_{ss} = 0 \text{ then } Y_{ss} &= \frac{\mu_W}{\mu_U} \end{aligned} \tag{10}$$

In other words, Y_{ss} is controlled to a reference value $\frac{\mu_W}{\mu_U}$, to which it returns exactly after any step perturbation to the system, provided that the steady-state exists and it is stable (see Olsman *et al.* [7] for further discussion). This conclusion is independent of the particular subsystem being controlled, W being inactive (Eq. 6) or active (Eq. 7) in the complex form, as well the active degradation rate (η_-), and complex formation dynamics ($\frac{d}{dt}C$).

S2.1 Understanding effect of saturation on modified antithetic feedback control

S2.1.1 ATF control limits with inactive complex

In this section we prove that for the system described in Eqs. 3-6, if $(\gamma + \gamma_W) > 0$, as Y-synthesis rate (μ_Y) value decreases, $\text{CoRa}_{\mu_Y \in \Theta}(\mu_Y) \to 1$. Similarly, if $(\gamma + \gamma_U) > 0$, as μ_Y increases, CoRa saturates with $\text{CoRa}_{\mu_Y \in \Theta}(\mu_Y) \to 0.5$. These analytically argued results are corroborated by computational demonstrations in Figure S4A.

Proposition 1. *For the system described in Eqs. 3-6, as $\mu_Y \to \mu'_Y$, $\Delta\log(Y_{ss}) = \Delta\log(\mu_Y) + \Delta\log(W_{ss})$. Here, for brevity, we denote $Y_{ss}|_{\Theta,\mu_Y}$ by Y_{ss}, and $Y_{ss}|_{\Theta,\mu'_Y}$ by Y'_{ss}, and similarly for W_{ss}. Therefore $\Delta\log(Y_{ss}) = \log(Y'_{ss}) - \log(Y_{ss})$, $\Delta\log(W_{ss}) = \log(W'_{ss}) - \log(W_{ss})$, and $\Delta\log(\mu_Y) = \log(\mu'_Y) - \log(\mu_Y)$.*

Proof. Given Eq. 6, the output steady state for the system is

$$Y_{ss} = \Big(\frac{\mu_Y}{\gamma + \gamma_Y}\Big) W_{ss} \tag{11}$$

After a perturbation $\mu_Y \to \mu'_Y$, the new output steady state can be written as

$$Y'_{ss} = \Big(\frac{\mu'_Y}{\gamma + \gamma_Y}\Big) W'_{ss} \tag{12}$$

Then, the effect of the perturbation on the system can be quantified as

$$\begin{aligned} \Delta\log(Y_{ss}) &= \log(Y'_{ss}) - \log(Y_{ss}) = \log\Big(\frac{Y'_{ss}}{Y_{ss}}\Big) \\ &= \log\Big(\frac{\big(\frac{\mu'_Y}{\gamma+\gamma_Y}\big)W'_{ss}}{\big(\frac{\mu_Y}{\gamma+\gamma_Y}\big)W_{ss}}\Big) = \log\Big(\Big(\frac{\mu'_Y}{\mu_Y}\Big)\Big(\frac{W'_{ss}}{W_{ss}}\Big)\Big) \\ &= \Delta\log(\mu_Y) + \Delta\log(W_{ss}) \end{aligned} \tag{13}$$

where the effect of the feedback is introduced by the $\Delta\log(W_{ss})$ component.

Consequence 1. In the absence of feedback (i.e. when U and the W do not depend on Y), W_{ss} should remain constant after a μ_Y-perturbation, i.e. $\Delta\log(W_{ss}) = 0$. Then, for this system, the effect of the step μ_Y perturbation is simply equal to the size of the perturbation, i.e. $\Delta\log(Y_{ss}) = \Delta\log(\mu_Y)$.

Consequence 2. By definition, a system has feedback control if the presence of feedback reduces the effect of the perturbation over the output change, i.e. $|\Delta\log(Y_{ss})| < |\Delta\log(\mu_Y)|$. Then, in order to have feedback control, $\Delta\log(W_{ss}) < 0$ if $\Delta\log(\mu_Y) > 0$ (and vice versa). It follows that in a range of μ_Y values with effective feedback control, W_{ss} must decrease monotonically as μ_Y value increases.

Proposition 2. *For the system described in Eqs. 3-6, if $(\gamma + \gamma_W) > 0$, the total W steady state ($W_{T,ss} = W_{ss} + C_{ss}$) has an upper limit and lower limit that is independent of μ_Y. Additionally, $W_{T,ss}$ approaches its upper limit when $W_{ss} \approx W_{T,ss}$, and its lower limit when $C_{ss} \approx W_{T,ss}$.*

Proof. Let's define total W as the sum of free molecule W and the complex molecule C, i.e. $W_T = W + C$. Then, the equation of change of W_T corresponds to the sum of Eq. 4 and Eq. 5:

$$\begin{aligned} \frac{d}{dt}W_T &= \frac{d}{dt}W + \frac{d}{dt}C \\ &= \mu_W - (\gamma + \gamma_W)(W + C) - \eta_- C \end{aligned} \tag{14}$$

Without loss of generality, we represent C as a fraction of the total W, αW_T with $\alpha \in [0, 1]$:

$$\frac{d}{dt}W_T = \mu_W - (\gamma + \gamma_W + \alpha\eta_-)W_T \tag{15}$$

Then, in steady state:

$$W_{T,ss} = \frac{\mu_W}{\gamma + \gamma_W + \alpha\eta_-} \tag{16}$$

Given that all involved parameters are non-negative, and $\alpha \in [0, 1]$:

$$\begin{aligned} \frac{\mu_W}{\gamma + \gamma_W + \eta_-} \leq &\ \frac{\mu_W}{\gamma + \gamma_W + \alpha\eta_-} \ \leq \frac{\mu_W}{\gamma + \gamma_W} \\ \frac{\mu_W}{\gamma + \gamma_W + \eta_-} \leq &\ W_{T,ss} \ \leq \frac{\mu_W}{\gamma + \gamma_W} \end{aligned} \tag{17}$$

Notice that the upper limit exists only if $(\gamma + \gamma_W) > 0$. Moreover, it is clear that $W_{T,ss}$ approaches its upper limit when $\alpha \to 0$, i.e. $W_{T,ss} \approx W_{ss}$, while $W_{T,ss}$ approaches its lower limit when $\alpha \to 1$, i.e. $W_{T,ss} \approx C_{ss}$.

Proposition 3. *For the system described in Eqs. 3-6, and within the range of μ_Y for which the feedback is effective (i.e. $|\Delta\log(Y_{ss})| < |\Delta\log(\mu_Y)|$ for all μ_Y values within the range),* $\mathrm{CoRa}_{\mu_Y \in \Theta}(\mu_Y) \to 1$ *as μ_Y decreases, provided that $(\gamma + \gamma_W) > 0$.*

Proof. As $W_{T,ss} = W_{ss} + C_{ss}$ is upper bounded (Eq. 17), W_{ss} must have an upper limit as well (i.e. its supremum, $\sup_{\mu_Y}(W_{ss}) \leq \frac{\mu_W}{\gamma + \gamma_W}$). By *Consequence 2* above, within the μ_Y range where feedback control is effective, W_{ss} value increases as the μ_Y value (before a perturbation is applied) decreases. Therefore, as μ_Y decreases, W_{ss} approaches its supremum, $\sup_{\mu_Y}(W_{ss})$. As this occurs, the increment to its concentration ($\Delta\log(W_{ss})$) after an additional perturbation that decreases the μ_Y value even further (i.e. $\Delta\log(\mu_Y) < 0$) is constrained by the W_{ss} proximity to its limit. With some abuse of notation, we use the symbol $\approx$ to denote the situation in which this limit is taken as W_{ss} approaches its upper bound. As a result, in this regime, $W_{ss} \approx \sup_{\mu_Y}(W_{ss})$ and $\Delta\log(W_{ss}) \approx 0$. Now, using Eq. 13 and *Consequence 1*,

$$\mathrm{CoRa}_{\mu_Y \in \Theta}(\mu_Y) = \frac{\Delta\log(\mathrm{Y_{ss}})}{\Delta\log(\mathrm{Y_{ss,NF}})}$$

$$
\begin{aligned}
&= \frac{\Delta\log(\mu_Y) + \Delta\log(W_{ss})}{\Delta\log(\mu_Y)} \\
&\approx \frac{\Delta\log(\mu_Y)}{\Delta\log(\mu_Y)} \qquad (18)\\
&\approx 1 \qquad (19)
\end{aligned}
$$

Proposition 4. *For the system described in Eqs. 3-6, and within the range of μ_Y for which the feedback is effective (i.e. $|\Delta\log(Y_{ss})| < |\Delta\log(\mu_Y)|$ for all μ_Y values within the range),* $\mathrm{CoRa}_{\mu_Y\in\Theta}(\mu_Y) \to 0.5$ *as μ_Y increases, provided that $(\gamma + \gamma_U) > 0$.*

Proof. By *Consequence 2* above, in a range of μ_Y values with feedback control, W_{ss} value decreases as the μ_Y value (before a perturbation is applied) increases. As $W_{T,ss} = W_{ss} + C_{ss}$ is lower bounded (Eq. 17), and $W_{T,ss}$ is minimal when C_{ss} approaches $W_{T,ss}$, C_{ss} must have an lower limit as well (i.e. its infimum, $\inf_{\mu_Y}(C_{ss}) \geq \frac{\mu_W}{\gamma+\gamma_W+\eta_-}$), and $C_{ss} \to \inf_{\mu_Y}(C_{ss})$ as μ_Y increases.

Let's define total U as the sum of free molecule U and the complex molecule C, i.e. $U_T = U + C$. Then, the equation of change of U_T corresponds to the sum of Eq. 3 and Eq. 5:

$$
\begin{aligned}
\frac{d}{dt}U_T &= \frac{d}{dt}U + \frac{d}{dt}C \\
&= \mu_U Y - (\gamma + \gamma_U)(U + C) - \eta_- C \qquad (20)\\
&= \mu_U Y - (\gamma + \gamma_U)U_T - \eta_- C \qquad (21)
\end{aligned}
$$

Let's assume that μ_Y is large enough such that C_{ss} approaches its lower bound, which is given by $c = \inf_{\mu_Y}(C_{ss})$. With some abuse of notation, we use the symbol $\approx$ to denote the situation in which this limit is taken as C_{ss} approaches its lower bound.

$$
U_{T,ss} \approx \frac{\mu_U Y_{ss} - \eta_- c}{\gamma + \gamma_U} \qquad (22)
$$

and

$$
\begin{aligned}
U_{ss} &\approx U_{T,ss} - c \\
&= \frac{\mu_U Y_{ss} - (\eta_- + \gamma + \gamma_U)c}{\gamma + \gamma_U} \qquad (23)
\end{aligned}
$$

Solving Eq. 5 in steady state, and substituting C_{ss}, U_{ss},

$$
\begin{aligned}
0 &= \eta_+ U_{ss} W_{ss} - (\gamma + \eta_0 + \eta_- + \gamma_U + \gamma_W)C_{ss} \\
W_{ss} &= \Big(\frac{\gamma + \eta_0 + \eta_- + \gamma_U + \gamma_W}{\eta_+}\Big)\Big(\frac{C_{ss}}{U_{ss}}\Big) \\
&= K_d\Big(\frac{C_{ss}}{U_{ss}}\Big) \\
&\approx K_d\Big(\frac{(\gamma + \gamma_U)c}{\mu_U Y_{ss} - (\eta_- + \gamma + \gamma_U)c}\Big) \qquad (24)
\end{aligned}
$$

with $K_d := \frac{\gamma+\eta_0+\eta_-+\gamma_U+\gamma_W}{\eta_+}$. Then, solving Eq. 6 in steady state, and substituting W_{ss},

$$
\begin{aligned}
0 &= \mu_Y W_{ss} - (\gamma + \gamma_Y)Y_{ss} \\
Y_{ss} &= \frac{\mu_Y}{\gamma + \gamma_Y} W_{ss} \\
Y_{ss} &\approx \Big(\frac{\mu_Y}{\gamma + \gamma_Y}\Big)\Big(\frac{K_d(\gamma + \gamma_U)c}{\mu_U Y_{ss} - (\eta_- + \gamma + \gamma_U)c}\Big) \\
0 &\approx Y_{ss}^2 - \Big(\frac{(\eta_- + \gamma + \gamma_U)c}{\mu_U}\Big)Y_{ss} - \Big(\frac{\mu_Y K_d(\gamma + \gamma_U)c}{\mu_U(\gamma + \gamma_Y)}\Big)
\end{aligned}
$$

$$
\begin{aligned}
Y_{ss} &\approx \Big(\frac{1}{2}\Big)\Big(\Big(\frac{(\eta_- + \gamma + \gamma_U)c}{\mu_U}\Big) + \sqrt{\Big(\frac{(\eta_- + \gamma + \gamma_U)c}{\mu_U}\Big)^2 + 4\Big(\frac{\mu_Y K_d(\gamma+\gamma_U)c}{\mu_U(\gamma+\gamma_Y)}\Big)}\Big) \\
&= \Big(\frac{(\eta_- + \gamma + \gamma_U)c}{2\mu_U}\Big)\Big(1 + \sqrt{1 + 4\Big(\frac{\mu_Y \mu_U K_d(\gamma+\gamma_U)}{(\gamma+\gamma_Y)(\eta_- + \gamma + \gamma_U)^2 c}\Big)}\Big) \\
&= \Big(\frac{(\eta_- + \gamma + \gamma_U)c}{2\mu_U}\Big)\Big(1 + \sqrt{1 + a \cdot \mu_Y}\Big) \qquad (25)
\end{aligned}
$$

with $a := 4\Big(\frac{\mu_U K_d(\gamma+\gamma_U)}{(\gamma+\gamma_Y)(\eta_- + \gamma + \gamma_U)^2 c}\Big)$. As a result, the change of the steady-state output Y_{ss} after a small perturbation on μ_Y ($\mu_Y \to \mu'_Y$, used to compute CoRa),

$$
\begin{aligned}
\Delta\log(Y_{ss}) &= \log\Big(\frac{\big(\frac{(\eta_- + \gamma + \gamma_U)c}{2\mu_U}\big)\big(1 + \sqrt{1 + a \cdot \mu'_Y}\big)}{\big(\frac{(\eta_- + \gamma + \gamma_U)c}{2\mu_U}\big)\big(1 + \sqrt{1 + a \cdot \mu_Y}\big)}\Big) \\
&= \log\Big(\frac{\big(1 + \sqrt{1 + a \cdot \mu'_Y}\big)}{\big(1 + \sqrt{1 + a \cdot \mu_Y}\big)}\Big) \qquad (26)
\end{aligned}
$$

On the other hand, given *Consequence 1*, the no-feedback system has $\Delta\log(Y_{ss,NF}) = \Delta\log(\mu_Y) = \log(\frac{\mu'_Y}{\mu_Y})$, and the associated CoRa value is given by:

$$
\mathrm{CoRa} = \frac{\log\Big(\frac{1+\sqrt{1+a\cdot\mu'_Y}}{1+\sqrt{1+a\cdot\mu_Y}}\Big)}{\log(\frac{\mu'_Y}{\mu_Y})} \qquad (27)
$$

As μ_Y increases, with $(a \cdot \mu_Y) \gg 1$, such that $(1 + \sqrt{1 + a \cdot \mu_Y}) \approx \sqrt{a \cdot \mu_Y}$, then

$$
\begin{aligned}
\mathrm{CoRa} &\approx \frac{\log\Big(\frac{(a\cdot\mu'_Y)^{0.5}}{(a\cdot\mu_Y)^{0.5}}\Big)}{\log(\frac{\mu'_Y}{\mu_Y})} \\
&\approx \frac{0.5\log(\frac{\mu'_Y}{\mu_Y})}{\log(\frac{\mu'_Y}{\mu_Y})} \\
&\approx 0.5 \qquad (28)
\end{aligned}
$$

S2.1.2 ATF control limits with active complex

In this section, we demonstate that for the system described in Eqs. 3-5,7, if $(\gamma + \gamma_W) > 0$, as Y-synthesis rate (μ_Y) value decreases, $\mathrm{CoRa}_{\mu_Y \in \Theta}(\mu_Y) \to 1$. Similarly, as μ_Y increases, CoRa saturates with $\mathrm{CoRa}_{\mu_Y \in \Theta}(\mu_Y) \to 1$, regardless of $\gamma, \gamma_W, \gamma_U = 0$. These analytically argued results are corroborated by computational demonstrations in Figure S4B.

Proposition 5. *For the system described on Eqs. 3-5,7, as $\mu_Y \to \mu'_Y$, $\Delta\log(Y_{ss}) = \Delta\log(\mu_Y) + \Delta\log(W_{T,ss})$. Here, for brevity, we denote $Y_{ss}|_{\Theta,\mu_Y}$ by Y_{ss}, and $Y_{ss}|_{\Theta,\mu'_Y}$ by Y'_{ss}, and similarly for $W_{T,ss}$. Therefore $\Delta\log(Y_{ss}) = \log(Y'_{ss}) - \log(Y_{ss})$, $\Delta\log(W_{T,ss}) = \log(W'_{T,ss}) - \log(W_{T,ss})$, and $\Delta\log(\mu_Y) = \log(\mu'_Y) - \log(\mu_Y)$.*

Proof. Given Eq. 7, the output steady state for the system is

$$
\begin{aligned}
Y_{ss} &= \Big(\frac{\mu_Y}{\gamma + \gamma_Y}\Big)(W_{ss} + C_{ss}) \\
&= \Big(\frac{\mu_Y}{\gamma + \gamma_Y}\Big)W_{T,ss} \qquad (29)
\end{aligned}
$$

After a perturbation $\mu_Y \to \mu'_Y$, the new output steady state can be written as

$$
Y'_{ss} = \Big(\frac{\mu'_Y}{\gamma + \gamma_Y}\Big)W'_{T,ss} \qquad (30)
$$

Then, the effect of the perturbation on the system can be quantified as

$$\begin{aligned}\Delta\log(Y_{ss}) &= \log(Y'_{ss}) - \log(Y_{ss}) = \log\Big(\frac{Y'_{ss}}{Y_{ss}}\Big) \\ &= \log\Big(\frac{\big(\frac{\mu'_Y}{\gamma+\gamma_Y}\big)W'_{T,ss}}{\big(\frac{\mu_Y}{\gamma+\gamma_Y}\big)W_{T,ss}}\Big) = \log\Big(\Big(\frac{\mu'_Y}{\mu_Y}\Big)\Big(\frac{W'_{T,ss}}{W_{T,ss}}\Big)\Big) \\ &= \Delta\log(\mu_Y) + \Delta\log(W_{T,ss}) \end{aligned} \tag{31}$$

where the effect of the feedback is introduced by the $\Delta\log(W_{T,ss})$ component.

Consequence 3. In the absence of feedback (i.e. when U and W do not depend on Y), $W_{T,ss}$ should remain constant after a μ_Y-perturbation, i.e. $\Delta\log(W_{T,ss}) = 0$. As a result, the effect of the perturbation on the system is simply equal to the size of the perturbation, i.e. $\Delta\log(Y_{ss}) = \Delta\log(\mu_Y)$.

Consequence 4. By definition, a system has feedback control if the presence of feedback reduces the effect of the perturbation over the output change, i.e. $|\Delta\log(Y_{ss})| < |\Delta\log(\mu_Y)|$. Then, in order to have feedback control, $\Delta\log(W_{T,ss}) < 0$ if $\Delta\log(\mu_Y) > 0$ (and vice versa). It follows that in range of μ_Y values with effective feedback control, $W_{T,ss}$ must decrease monotonically as μ_Y value increases.

Proposition 6. *For the system described in Eqs. 3-5,7, if $(\gamma + \gamma_W) > 0$, the total W steady state ($W_{T,ss} = W_{ss} + C_{ss}$) has an upper limit and lower limit, independent of μ_Y. Additionally, $W_{T,ss}$ approaches its upper limit when $W_{ss} \approx W_{T,ss}$, and its lower limit when $C_{ss} \approx W_{T,ss}$.*

Proof. Let's define total W as the sum of free molecule W and the complex molecule C, i.e. $W_T = W + C$. Then, the equation of change of W_T corresponds to the sum of Eq. 4 and Eq. 5:

$$\begin{aligned}\frac{d}{dt}W_T &= \frac{d}{dt}W + \frac{d}{dt}C \\ &= \mu_W - (\gamma + \gamma_W)(W + C) - \eta_- C \end{aligned} \tag{32}$$

Without loss of generality, we represent C as a fraction of the total W, αW_T with $\alpha \in [0, 1]$:

$$\frac{d}{dt}W_T = \mu_W - (\gamma + \gamma_W + \alpha\eta_-)W_T \tag{33}$$

Then, at steady state:

$$W_{T,ss} = \frac{\mu_W}{\gamma + \gamma_W + \alpha\eta_-} \tag{34}$$

Given that all involved parameters are non-negative, and $\alpha \in [0, 1]$:

$$\begin{aligned}\frac{\mu_W}{\gamma + \gamma_W + \eta_-} \leq &\ \frac{\mu_W}{\gamma+\gamma_W+\alpha\eta_-} \ \leq \frac{\mu_W}{\gamma + \gamma_W} \\ \frac{\mu_W}{\gamma + \gamma_W + \eta_-} \leq &\ W_{T,ss} \ \leq \frac{\mu_W}{\gamma + \gamma_W}\end{aligned} \tag{35}$$

Notice that the upper limit exists only if $(\gamma + \gamma_W) > 0$. Moreover, it is clear that $W_{T,ss}$ approaches its upper limit when $\alpha \to 0$, i.e. $W_{T,ss} \approx W_{ss}$, while $W_{T,ss}$ approaches its lower limit when $\alpha \to 1$, i.e. $W_{T,ss} \approx C_{ss}$.

Proposition 7. *For the system described in Eqs. 3-5,7 and within the range of μ_Y for which the feedback is effective (i.e. $|\Delta\log(Y_{ss})| < |\Delta\log(\mu_Y)|$), $\mathrm{CoRa}_{\mu_Y\in\Theta}(\mu_Y) \to 1$ as μ_Y decreases, provided that $(\gamma + \gamma_W) > 0$.*

Proof. By *Consequence 4*, in the range of effective feedback control, $W_{T,ss}$ value increases as the μ_Y value (before a perturbation is applied) decreases. Therefore, as the μ_Y value decreases, $W_{T,ss}$ approaches its limit, $\frac{\mu_W}{\gamma+\gamma_W}$ (Eq. 35). Therefore, the potential increment to its concentration ($\Delta\log(W_{T,ss})$) after a perturbation that decreases μ_Y value

even further (i.e. $\Delta\log(\mu_Y) < 0$) is constrained by the $W_{T,ss}$ proximity to the limit. With some abuse of notation, we use the symbol $\approx$ to denote the situation in which the limit is taken as W_{ss} approaches its upper bound. In this regime, $W_{T,ss} \approx \frac{\mu_W}{\gamma+\gamma_W}$ and $\Delta\log(W_{ss}) \approx 0$. Using Eq. 31 and *Consequence 3*,

$$\begin{aligned}
\mathrm{CoRa}_{\mu_Y\in\Theta}(\mu_Y) &= \frac{\Delta\log(\mathrm{Y_{ss}})}{\Delta\log(\mathrm{Y_{ss,NF}})} \\
&= \frac{\Delta\log(\mu_\mathrm{Y}) + \Delta\log(\mathrm{W_{T,ss}})}{\Delta\log(\mu_\mathrm{Y})} \\
&\approx \frac{\Delta\log(\mu_\mathrm{Y})}{\Delta\log(\mu_\mathrm{Y})} \\
&\approx 1
\end{aligned} \tag{36}$$

Proposition 8. *For the system described in Eqs. 3-5,7, and within a range in which the feedback is effective (i.e.* $|\Delta\log(Y_{ss})| < |\Delta\log(\mu_Y)|$ *for all* μ_Y *values within the range),* $\mathrm{CoRa}_{\mu_Y\in\Theta}(\mu_Y) \to 1$ *as* μ_Y *increases.*

Proof. By *Consequence 4* above, in a range of μ_Y values with effective feedback control, $W_{T,ss}$ value decreases as the μ_Y value (before a perturbation is applied) increases. Therefore, as the μ_Y value increases, $W_{T,ss}$ approaches its limit, $\frac{\mu_W}{\gamma+\gamma_W+\eta_-}$ (Eq. 35). Then the potential reduction on its concentration ($\Delta\log(W_{T,ss})$) after a perturbation that increases μ_Y value even further (i.e. $\Delta\log(\mu_Y) > 0$) is constrained by the $W_{T,ss}$ proximity to the limit. Then as the μ_Y value (before a perturbation is applied) increases, such that $W_{T,ss} \approx \frac{\mu_W}{\gamma+\gamma_W+\eta_-}$ and $\Delta\log(W_{ss}) \approx 0$ (with the same abuse of notation highlighted above as to limits), using Eq. 31 and *Consequence 3*,

$$\begin{aligned}
\mathrm{CoRa}_{\mu_Y\in\Theta}(\mu_Y) &= \frac{\Delta\log(\mathrm{Y_{ss}})}{\Delta\log(\mathrm{Y_{ss,NF}})} \\
&= \frac{\Delta\log(\mu_\mathrm{Y}) + \Delta\log(\mathrm{W_{T,ss}})}{\Delta\log(\mu_\mathrm{Y})} \\
&\approx \frac{\Delta\log(\mu_\mathrm{Y})}{\Delta\log(\mu_\mathrm{Y})} \\
&\approx 1
\end{aligned} \tag{37}$$

Notice this limit exists even if W and U are lost only through their mutual annihilation (i.e. $\gamma, \gamma_W, \gamma_U = 0$), as the active degradation is not spontaneous (i.e. $0 < \eta_- < \infty$).

S2.2 Limits and the controlled system

It must be emphasized that the control limits described above depend directly on the specific subsystem being controlled, and that analytical intuitive expressions might not always be feasible. CoRa has the advantage of not having to rely on this knowledge. In this paper, we also analyze three different controlled subsystems with the antithetic feedback control (ATF), for which no clear analytical derivations are possible :

1. One-step subsystem:

$$\frac{d}{dt}Y = \mu_Y W - (\gamma+\gamma_Y)Y \tag{38}$$

2. Double-negative subsystem:

$$\begin{aligned}
\frac{d}{dt}Y_0 &= \mu_0 W - (\gamma+\gamma_Y)Y_0 \\
\frac{d}{dt}Y_1 &= \mu_1 \frac{K_1}{Y_0+K_1} - (\gamma+\gamma_Y)Y_1 \\
\frac{d}{dt}Y &= \mu_Y \frac{K_D}{Y_1+K_D} - (\gamma+\gamma_Y)Y
\end{aligned} \tag{39}$$

3. Subsystem with positive feedback:

$$\begin{aligned}\frac{d}{dt}Y_0 &= \mu_0 W - (\gamma+\gamma_Y)Y_0\\ \frac{d}{dt}Y_1 &= \mu_1 Y_0 + \mu_P \frac{Y_1}{Y_1+K_P} - (\gamma+\gamma_Y)Y_1\\ \frac{d}{dt}Y &= \mu_Y Y_1 - (\gamma+\gamma_Y)Y \end{aligned} \tag{40}$$

In all cases, W induces the synthesis of the subsystem, and Y is the output of interest, as well as the feedback input (Eqs. 3-5; Fig. S2). Choosing Y as the system's output, the corresponding locally analogous system without feedback maintains the same ODE equations except for the input to the control subsystem (U synthesis induction for the ATF examples), where Y is substituted by a new molecule Y_*, which is constitutively expressed such that the steady state output of the locally analogous system without feedback $Y_{ss,NF}$ is equal to the steady state output of the feedback system Y_{ss} (i.e. Y_* degradation rate $\gamma_{Y*}=\gamma_Y$, and Y_* synthesis rate, $\mu_{Y*}=\mu_Y W_{ss}$, $\mu_{Y*}=\mu_Y\frac{K_D}{Y_{1,ss}+K_D}$, or $\mu_{Y*}=\mu_Y Y_{1,ss}$, depending on the subsystem being considered).

Even with these simple examples, we observed that depending on the subsystem being controlled, the exact same control motif has not only different performance, but qualitatively different responses to the tuning of the control parameters (Fig. S2).

S3 Understanding effect of saturation on buffering + negative feedback control strategy

System proposed in Hancock *et al.* (2017) Hancock *et al.* (2017) explored a simple model proposed to display perfect adaptation. This system consisted of only two species, one working as a buffer of the other while inhibiting its own synthesis (i.e. negative feedback). The equations of this control strategy with a the simple controlled subsystem used in this paper are:

$$\frac{d}{dt}Y = (\mu_Y - kY) - \beta Y + \beta_P U_P - \gamma_Y Y \tag{41}$$

$$\frac{d}{dt}U_P = \beta Y - \beta_P U_P - \gamma_{U_P} U_P \tag{42}$$

where μ_Y is the maximum synthesis rate of Y, β and β_P are inactivation and activation rates respectively, U_P represents the inactive form of Y, γ_Y and γ_{U_P} are the degradation rates of Y and U_P, respectively, and k is inhibition rate of Y over its own synthesis.

At steady state,

$$U_{P,ss} = \frac{\beta Y_{ss}}{\beta_P+\gamma_{U_P}} \tag{43}$$

$$Y_{ss} = \frac{\mu_Y}{k+\beta-\beta\frac{\beta_P}{\beta_P+\gamma_{U_P}}+\gamma_Y} \tag{44}$$

Then, assuming $\beta_P \gg \gamma_{U_P}$, Y_{ss} is controlled with a reference value $\frac{\mu_Y}{k+\gamma_Y}$.

We consider a modified implementation of this buffering + negative feedback (BNF v1) control motif where the feedback has an additional intermediate step:

$$\frac{d}{dt}Y = \mu_Y U - (\gamma+\gamma_Y)Y \tag{45}$$

$$\frac{d}{dt}U = f(Y) - (\gamma+\gamma_U)U - \beta U + \beta_P U_P \tag{46}$$

$$\frac{d}{dt}U_P = -(\gamma+\gamma_{U_P})U_P + \beta U - \beta_P U_P \tag{47}$$

The steady state solution for U and U_P is:

$$U_{ss} = Y_{ss}\Big(\frac{\gamma+\gamma_Y}{\mu_Y}\Big) \tag{48}$$

$$U_{P,ss} = \frac{\beta U_{ss}}{\gamma+\gamma_{U_P}+\beta_P} \tag{49}$$

For Y, in the case where $f(Y)=\mu_U - kY$ is a linear function:

$$Y_{ss} = \mu_U \frac{\mu_Y}{\mu_Y k + (\gamma+\gamma_U+\beta)(\gamma+\gamma_Y) - \beta(\gamma+\gamma_Y)\frac{\beta_P}{\gamma+\gamma_{U_P}+\beta_P}} \tag{50}$$

If we assume that $\gamma+\gamma_{U_P}\approx 0$, then Eq. 50 is reduced to:

$$Y_{ss} = \mu_U \frac{\mu_Y}{\mu_Y k + (\gamma+\gamma_U)(\gamma+\gamma_Y)} \tag{51}$$

The system has perfect adaptation only if $\mu_Y k \gg (\gamma+\gamma_U)(\gamma+\gamma_Y)$, in which case the reference value is $\frac{\mu_U}{k}$.

In the case where $f(Y)=\mu_U\frac{K_D}{K_D+Y}$ is a Michaelis-Menten function, steady state solution for Y is:

$$\begin{aligned} Y_{ss} &= \frac{-K_D+\sqrt{K_D^2+4K_D\Big(\frac{\mu_Y}{\gamma+\gamma_Y}\Big)\Big(\frac{\mu_U}{\gamma+\gamma_U}\Big)\Big(\frac{\gamma+\gamma_U+\beta_P}{\beta+\gamma+\gamma_U+\beta_P}\Big)}}{2} \\ &= \Big(\frac{K_D}{2}\Big)(-1+\sqrt{1+a\cdot\mu_Y}) \end{aligned} \tag{52}$$

with $a := \Big(\frac{4}{K_D}\Big)\Big(\frac{1}{\gamma+\gamma_Y}\Big)\Big(\frac{\mu_U}{\gamma+\gamma_U}\Big)\Big(\frac{\gamma+\gamma_U+\beta_P}{\beta+\gamma+\gamma_U+\beta_P}\Big)$. This steady state expression already suggests that perturbations to μ_Y cannot be perfectly controlled anymore. Moreover, we show below that regardless of the parameter values, BNF v1 with a Michaelis-Menten function describing the negative regulation has $\mathrm{CoRa}_{\theta\in\Theta}(\mu_Y)>0.5$.

The corresponding locally analogous system without feedback maintains the same ODE equations (Eq. 45 and Eq. 47), with the exception of $\frac{dU}{dt}$,

$$\frac{d}{dt}U = f(Y_*) - (\gamma+\gamma_U)U - \beta U + \beta_P U_P \tag{53}$$

where U synthesis rate now depends on a new molecule Y_* with dynamics

$$\frac{d}{dt}Y_* = \mu_{Y*} - (\gamma+\gamma_{Y*})Y_* \tag{54}$$

such that, for each parameter set Θ, Y_* is constitutively expressed with synthesis μ_{Y*} equal to Y synthesis rate in the pre-perturbation steady state solution (i.e. $\mu_{Y*}=\mu_Y U$), and degradation rate $\gamma_{Y*}=\gamma_Y$. Then, with $f(Y_*)=\mu_Y\frac{K_D}{K_D+Y_*}$, the output steady state solution $Y_{ss,NF}$ for this locally analogous system without feedback is:

$$\begin{aligned} Y_{ss,NF} &= \Big(\frac{K_D}{(\frac{\mu_{Y*}}{\gamma+\gamma_{Y*}})+K_D}\Big)\Big(\frac{\mu_Y}{\gamma+\gamma_Y}\Big)\Big(\frac{\mu_U}{\gamma+\gamma_U}\Big)\Big(\frac{\gamma+\gamma_U+\beta_P}{\beta+\gamma+\gamma_U+\beta_P}\Big) \\ &= \Big(\frac{K_D(\gamma+\gamma_{Y*})}{\mu_{Y*}+K_D(\gamma+\gamma_{Y*})}\Big)\Big(\frac{K_D}{4}\Big)\cdot a\cdot\mu_Y \end{aligned} \tag{55}$$

Control limits Using Eq. 52 and Eq. 55, the CoRa value for a small perturbation on μ_Y ($\mu_Y\to\mu_Y'$) is calculated as,

$$\begin{aligned} \mathrm{CoRa}_{\mu_Y\in\Theta}(\mu_Y) &= \frac{\log\Big(\frac{(\frac{K_D}{2})(-1+\sqrt{1+a\cdot\mu_Y'})}{(\frac{K_D}{2})(-1+\sqrt{1+a\cdot\mu_Y})}\Big)}{\log\Big(\frac{(\frac{K_D(\gamma+\gamma_{Y*})}{\mu_{Y*}+K_D(\gamma+\gamma_{Y*})})(\frac{K_D}{4})a\cdot\mu_Y'}{(\frac{K_D(\gamma+\gamma_{Y*})}{\mu_{Y*}+K_D(\gamma+\gamma_{Y*})})(\frac{K_D}{4})a\cdot\mu_Y}\Big)} \\ &= \frac{\log\Big(\frac{-1+\sqrt{1+a\cdot\mu_Y'}}{-1+\sqrt{1+a\cdot\mu_Y}}\Big)}{\log(\frac{\mu_Y'}{\mu_Y})} \end{aligned} \tag{56}$$

First, we show that $\text{CoRa}_{\mu_Y\in\Theta}(\mu_Y)$ decreases monotonically as the μ_Y value (before the perturbation) increases (i.e. $d\text{CoRa}_{\mu_Y\in\Theta}(\mu_Y)/d\mu_Y < 0$). In order to evaluate the derivative of CoRa, we first need to derive the continuous form of the CoRa function (CoRa^C), which corresponds to CoRa evaluated in the limit as the perturbation size ($\Delta\mu_Y$, with $\mu'_Y = \mu_Y + \Delta\mu_Y$) approaches zero,

$$\begin{aligned}
\text{CoRa}^C_{\mu_Y\in\Theta}(\mu_Y) &= \lim_{\Delta\mu_Y\to 0}(\text{CoRa}_{\mu_Y\in\Theta}(\mu_Y)) \\
&= \frac{\log\Big(\frac{-1+\sqrt{1+a\cdot(\mu_Y+\Delta\mu_Y)}}{-1+\sqrt{1+a\cdot\mu_Y}}\Big)}{\log(\frac{(\mu_Y+\Delta\mu_Y)}{\mu_Y})}|_{\lim_{\Delta\mu_Y\to 0}} \\
&= \frac{\log(-1+\sqrt{1+a\cdot(\mu_Y+\Delta\mu_Y)}) - \log(-1+\sqrt{1+a\cdot\mu_Y})}{\log((\mu_Y+\Delta\mu_Y)) - \log(\mu_Y)}|_{\lim_{\Delta\mu_Y\to 0}} \\
&= \frac{\frac{\log(-1+\sqrt{1+a\cdot(\mu_Y+\Delta\mu_Y)})-\log(-1+\sqrt{1+a\cdot\mu_Y})}{\Delta\mu_Y}}{\frac{\log((\mu_Y+\Delta\mu_Y))-\log(\mu_Y)}{\Delta\mu_Y}}|_{\lim_{\Delta\mu_Y\to 0}} \\
&= \frac{\frac{d}{d\mu_Y}\log(-1+\sqrt{1+a\cdot\mu_Y})}{\frac{d}{d\mu_Y}\log(\mu_Y)} \\
&= \frac{1}{2}\Big(1+\frac{1}{\sqrt{1+a\cdot\mu_Y}}\Big)
\end{aligned} \tag{57}$$

Then,

$$\begin{aligned}
\frac{d}{d\mu_Y}\text{CoRa}^C_{\mu_Y\in\Theta}(\mu_Y) &= \frac{d}{d\mu_Y}\Big(\frac{1}{2}\Big(1+\frac{1}{\sqrt{1+a\cdot\mu_Y}}\Big) \\
&= -\frac{a}{4(1+a\cdot\mu_Y)^{\frac{3}{2}}} < 0
\end{aligned} \tag{58}$$

As all parameters are positive (i.e. $a > 0$ and $\mu_Y > 0$), this derivative is always negative.

From Eq. 56, it is easy to see that as the μ_Y value (before the perturbation) increases, with $(a\cdot\mu_Y) \gg 1$, such that $(-1+\sqrt{1+a\cdot\mu_Y}) \approx \sqrt{a\cdot\mu_Y}$, then

$$\begin{aligned}
\text{CoRa}_{\mu_Y\in\Theta}(\mu_Y) &\approx \frac{\log\Big(\frac{(a\cdot\mu'_Y)^{0.5}}{(a\cdot\mu_Y)^{0.5}}\Big)}{\log(\frac{\mu'_Y}{\mu_Y})} \\
&\approx \frac{0.5\log(\frac{\mu'_Y}{\mu_Y})}{\log(\frac{\mu'_Y}{\mu_Y})} \\
&\approx 0.5
\end{aligned} \tag{59}$$

It follows that regardless of the parameter values, BNF v1 with a Michaelis-Menten function describing the negative synthesis regulation has $\text{CoRa}_{\mu_Y\in\Theta}(\mu_Y) > 0.5$.

S4 Comparing Feedback Control Morifs with CoRa

For all systems below, Y represents the system output.

S4.1 Antithetic Feedback

We consider a simple version of the Antithetic Feedback motif (ATF) proposed by Briat *et al.* [2], where Y is being produced at a rate that depends on the concentration of W, while U synthesis is induced by Y, which then binds W,

forming a transitory complex C, which eventually leads to the mutual degradation of U and W:

$$\frac{d}{dt}U = \mu_U Y - (\gamma + \gamma_U)U - \eta_+ UW + (\eta_0 + \gamma_W)C \quad (60)$$

$$\frac{d}{dt}W = \mu_W - (\gamma + \gamma_W)W - \eta_+ UW + (\eta_0 + \gamma_U)C \quad (61)$$

$$\frac{d}{dt}C = \eta_+ UW - (\gamma + \eta_0 + \eta_- + \gamma_U + \gamma_W)C \quad (62)$$

For Y dynamics, two alternative scenarios can be easily foreseen: W can be either inactivated as a transcription factor once it binds U (ATF v1; Fig. 3A),

$$\frac{d}{dt}Y = \mu_Y W - (\gamma + \gamma_Y)Y \quad (63)$$

or W retains its transcription factor activity until degraded (ATF v2; Fig. 3D),

$$\frac{d}{dt}Y = \mu_Y (W + C) - (\gamma + \gamma_Y)Y \quad (64)$$

Here all species are subject to loss by dilution (γ), in addition of their own individual degradation rates ($\gamma_\square$), $\mu_\square$ represents the synthesis rate for each molecule (either constitutive, μ_W, or dependent of the associated transcription factor, μ_U and μ_Y), and η_- is the co-degradation rate of U, W in the complex form C; η_+ is the binding rate of U and W (forming the complex C); and η_0 is the spontaneous unbinding rate of these two molecules (dissociating the complex C).

The corresponding locally analogous system without feedback maintains the same ODE equations (Eq. 61-62, and either Eq. 63 or Eq. 64), with the exception of $\frac{dU}{dt}$,

$$\frac{d}{dt}U = \mu_U Y_* - (\gamma + \gamma_U)U - \eta_+ UW + (\eta_0 + \gamma_W)C \quad (65)$$

where U synthesis rate now depends on a new molecule Y_* with dynamics

$$\frac{d}{dt}Y_* = \mu_{Y_*} - (\gamma + \gamma_{Y_*})Y_* \quad (66)$$

For each parameter set Θ, Y_* is constitutively expressed with synthesis μ_{Y*} equal to Y synthesis rate in the pre-perturbation steady state solution (i.e. either $\mu_{Y*} = \mu_Y W_{ss}$ or $\mu_{Y*} = \mu_Y (W_{ss} + C_{ss})$, depending on the feedback system being considered), and degradation rate $\gamma_{Y*} = \gamma_Y$.

S4.2 Feedback by Active Degradation

We consider a simple version of the Feedback by Active Degradation motif (FAD; [6, 9]), where Y is being produced at a rate that depends on the concentration of W, while U synthesis is induced by Y. Y then binds W, forming a transitory complex C, which eventually leads to the degradation of only W while freeing U:

$$\frac{d}{dt}U = \mu_U Y - (\gamma + \gamma_U)U - \eta_+ UW + (\eta_0 + \gamma_W + \eta_-)C \quad (67)$$

$$\frac{d}{dt}W = \mu_W - (\gamma + \gamma_W)W - \eta_+ UW + (\eta_0 + \gamma_U)C \quad (68)$$

$$\frac{d}{dt}C = \eta_+ UW - (\gamma + \eta_0 + \eta_- + \gamma_U + \gamma_W)C \quad (69)$$

For Y dynamics, two alternative scenarios can be easily foreseen: W can be either inactivated as a transcription factor once it binds U (FAD v1; Fig. 3B),

$$\frac{d}{dt}Y = \mu_Y W - (\gamma + \gamma_Y)Y \quad (70)$$

or W retains its transcription factor activity until degraded (FAD v2; Fig. 3E),

$$\frac{d}{dt}Y = \mu_Y(W+C) - (\gamma+\gamma_Y)Y \tag{71}$$

Here all species are subject to loss by dilution (γ), in addition of their own individual degradation rates ($\gamma_\square$), $\mu_\square$ represents the synthesis rate for each molecule (either constitutive, μ_W, or dependent of the associated transcription factor, μ_U and μ_Y), and η_- is the active degradation rate of W in the complex form C; η_+ is the binding rate of U and W (forming the complex C); and η_0 is the spontaneous unbinding rate of these two molecules (dissociating the complex C).

The corresponding locally analogous system without feedback maintains the same ODE equations (Eq. 68-69, and either Eq. 70 or Eq. 71), with the exception of $\frac{dU}{dt}$,

$$\frac{d}{dt}U = \mu_U Y_* - (\gamma+\gamma_U)U - \eta_+ UW + (\eta_0+\gamma_W+\eta_-)C \tag{72}$$

where U synthesis rate now depends on a new molecule Y_* with dynamics

$$\frac{d}{dt}Y_* = \mu_{Y_*} - (\gamma+\gamma_{Y_*})Y_* \tag{73}$$

For each parameter set Θ, Y_* is constitutively expressed with synthesis μ_{Y*} equal to Y synthesis rate in the pre-perturbation steady state solution (i.e. either $\mu_{Y*} = \mu_Y W_{ss}$ or $\mu_{Y*} = \mu_Y(W_{ss}+C_{ss})$, depending on the feedback system being considered), and degradation rate $\gamma_{Y*} = \gamma_Y$.

S4.3 Feedback by Active Degradation + Positive Feedback with inactive complex

We consider the FAD motif with the addition of a positive feedback (FDP; [3, 9]), i.e. W induces its own synthesis. Once again, two alternative scenarios can be easily foreseen: W can be either inactivated as a transcription factor once it binds U (FDP v1; Fig. 3C),

$$\frac{d}{dt}U = \mu_U Y - (\gamma+\gamma_U)U - \eta_+ UW + (\eta_0+\gamma_W+\eta_-)C \tag{74}$$

$$\frac{d}{dt}W = \mu_W\Big(\frac{W}{W+K_D}\Big) - (\gamma+\gamma_W)W - \eta_+ UW + (\eta_0+\gamma_U)C \tag{75}$$

$$\frac{d}{dt}C = \eta_+ UW - (\gamma+\eta_0+\eta_-+\gamma_U+\gamma_W)C \tag{76}$$

$$\frac{d}{dt}Y = \mu_Y W - (\gamma+\gamma_Y)Y \tag{77}$$

or W retains its transcription factor activity until degraded (FDP v2; Fig. 3F),

$$\frac{d}{dt}U = \mu_U Y - (\gamma+\gamma_U)U - \eta_+ UW + (\eta_0+\gamma_W+\eta_-)C \tag{78}$$

$$\frac{d}{dt}W = \mu_W\Big(\frac{(W+C)}{(W+C)+K_D}\Big) - (\gamma+\gamma_W)W - \eta_+ UW + (\eta_0+\gamma_U)C \tag{79}$$

$$\frac{d}{dt}C = \eta_+ UW - (\gamma+\eta_0+\eta_-+\gamma_U+\gamma_W)C \tag{80}$$

$$\frac{d}{dt}Y = \mu_Y(W+C) - (\gamma+\gamma_Y)Y \tag{81}$$

Here all species are subject to loss by dilution (γ), in addition of their own individual degradation rates ($\gamma_\square$), $\mu_\square$ represents the synthesis rate for each molecule, K_D is the Michaelis-Menten constant for W auto-regulation, and η_- is the active degradation rate of W in the complex form C; η_+ is the binding rate of U and W (forming the complex C); and η_0 is the spontaneous unbinding rate of these two molecules (dissociating the complex C).

The corresponding locally analogous system without feedback maintains the same ODE equations (either Eq. 75-77, or Eq. 79-81), with the exception of $\frac{dU}{dt}$,

$$\frac{d}{dt}U = \mu_U Y_* - (\gamma + \gamma_U)U - \eta_+ UW + (\eta_0 + \gamma_W + \eta_-)C \tag{82}$$

where U synthesis rate now depends on a new molecule Y_* with dynamics

$$\frac{d}{dt}Y_* = \mu_{Y_*} - (\gamma + \gamma_{Y_*})Y_* \tag{83}$$

For each parameter set Θ, Y_* is constitutively expressed with synthesis μ_{Y*} equal to Y synthesis rate in the pre-perturbation steady state solution (i.e. either $\mu_{Y*} = \mu_Y W_{ss}$ or $\mu_{Y*} = \mu_Y(W_{ss} + C_{ss})$, depending on the feedback system being considered), and degradation rate $\gamma_{Y*} = \gamma_Y$.

S4.4 Buffering + Negative Feedback

We consider a motif with negative feedback and a buffering loop (BNF v1 & v2; Fig. 3G-H), similar to the one proposed in Hancock *et al.* [4], where Y represses the synthesis of U, and U transitions to an alternative state U_P and vice versa:

$$\frac{d}{dt}U = \mu_U\Big(\frac{K_D}{Y + K_D}\Big) - (\gamma + \gamma_U)U - \beta U + \beta_P U_P \tag{84}$$

$$\frac{d}{dt}U_P = -(\gamma + \gamma_U)U_P + \beta U - \beta_P U_P \tag{85}$$

closing the feedback with either U inducing Y synthesis (BNF v1; Fig. 3G),

$$\frac{d}{dt}Y = \mu_Y U - (\gamma + \gamma_Y)Y \tag{86}$$

or U_P inducing Y synthesis (BNF v2; Fig. 3H):

$$\frac{d}{dt}Y = \mu_Y U_P - (\gamma + \gamma_Y)Y \tag{87}$$

Here all species are subject to loss by dilution (γ), in addition of their own individual degradation rates (γ_Y for Y, and γ_U for both U and U_P), μ_U is the maximum synthesis rate of U (in absence of Y), μ_Y is the synthesis rate of Y (depending either on U, Eq. 86, or U_P, Eq. 87), and β, β_P are the transition rates from U to U_P, and viceversa.

The corresponding locally analogous system without feedback maintains the same ODE equations (Eq. 85, and either Eq. 86 or Eq. 87), with the exception of $\frac{dU}{dt}$,

$$\frac{d}{dt}U = \mu_U\Big(\frac{K_D}{Y_* + K_D}\Big) - (\gamma + \gamma_U)U - \beta U + \beta_P U_P \tag{88}$$

where U synthesis rate now depends on a new molecule Y_* with dynamics

$$\frac{d}{dt}Y_* = \mu_{Y_*} - (\gamma + \gamma_{Y_*})Y_* \tag{89}$$

For each parameter set Θ, Y_* is constitutively expressed with synthesis μ_{Y*} equal to Y synthesis rate in the pre-perturbation steady state solution (i.e. either (i.e. either $\mu_{Y*} = \mu_Y U_{ss}$ or $\mu_{Y*} = \mu_Y U_{P,ss}$, depending on the feedback system being considered), and degradation rate $\gamma_{Y*} = \gamma_Y$.

S4.5 Feedback + Feedforward Loop

We consider a motif with negative feedback and a coherent feed-forward loop (FFL; Fig. 3H), similar to the one proposed in Harris *et al.* [5], where Y represses the synthesis of U, and U induces the synthesis of both Y and W, which in turns also induces Y synthesis:

$$\frac{d}{dt}U = \mu_U\Big(\frac{K_D}{Y+K_D}\Big) - (\gamma+\gamma_U)U \tag{90}$$

$$\frac{d}{dt}W = \mu_W U - (\gamma+\gamma_W)W \tag{91}$$

$$\frac{d}{dt}Y = \mu_Y(U+W) - (\gamma+\gamma_Y)Y \tag{92}$$

Here all species are subject to loss by dilution (γ), in addition of their own individual degradation rates ($\gamma_\square$), and $\mu_\square$ represents the synthesis rate for each molecule.

The corresponding locally analogous system without feedback maintains the same ODE equations (Eq. 91-92), with the exception of $\frac{dU}{dt}$,

$$\frac{d}{dt}U = \mu_U\Big(\frac{K_D}{Y_*+K_D}\Big) - (\gamma+\gamma_U)U \tag{93}$$

where U synthesis rate now depends on a new molecule Y_* with dynamics

$$\frac{d}{dt}Y_* = \mu_{Y_*} - (\gamma+\gamma_{Y_*})Y_* \tag{94}$$

For each parameter set Θ, Y_* is constitutively expressed with synthesis μ_{Y*} equal to Y synthesis rate in the pre-perturbation steady state solution (i.e. $\mu_{Y*} = \mu_Y(U_{ss}+W_{ss})$), and degradation rate $\gamma_{Y*} = \gamma_Y$.

S4.6 Brink Motif Feedback

We consider a simple version of the Brink motif (BMF) proposed by Samaniego & Franco [8], where A and I bind and annihilate each other (by creating the complex C), A induces the activation of U (U_P to U), while I induces its inactivation (U to U_P), and U induces the synthesis of Y:

$$\frac{d}{dt}C = -\gamma C + \eta_+ AI - \eta_0 C + \beta_A AU_P \tag{95}$$

$$\frac{d}{dt}U = \mu_U - \gamma U + \beta_A AU_P - \beta_I IU \tag{96}$$

$$\frac{d}{dt}U_P = -\gamma U_P - \beta_A AU_P + \beta_I IU \tag{97}$$

$$\frac{d}{dt}Y = \mu_Y U - (\gamma+\gamma_Y)Y \tag{98}$$

With Y either inducing the synthesis of I (BMF v1; Fig. 3I),

$$\frac{d}{dt}A = \mu_A - \gamma A - \eta_+ AI + \eta_0 C - \beta_A AU_P \tag{99}$$

$$\frac{d}{dt}I = \mu_I Y - \gamma B - \eta_+ AI + \eta_0 C - \beta_I IU \tag{100}$$

or Y repressing the synthesis of A (BMF v2; Fig. 3J),

$$\frac{d}{dt}A = \mu_A\Big(\frac{K_D}{Y+K_D}\Big) - \gamma A - \eta_+ AI + \eta_0 C - \beta_A AU_P \tag{101}$$

$$\frac{d}{dt}I = \mu_I - \gamma B - \eta_+ AI + \eta_0 C - \beta_I IU \tag{102}$$

Here all species are subject to loss by dilution (γ), $\mu_\square$ represents the synthesis rate for each molecule (except U_P, which is only created by the inactivation of U), η_+ is the binding rate of A and I (forming the complex C), η_0 is the spontaneous unbinding rate of these two molecules (dissociating the complex C); and β_A, β_I are the activation and inactivation rates of U, respectively. Finally, K_D is the Michaelis-Menten constant for the transcriptional repression by Y on Eq. 102.

The corresponding locally analogous system without feedback maintains the same ODE equations (Eq. 95-97, and either Eq. 99 or Eq. 102), with the exception of $\frac{dI}{dt}$ for BMF v1,

$$\frac{d}{dt}I = \mu_I Y_* - \gamma B - \eta_+ AI + \eta_0 C - \beta_I IU \tag{103}$$

or $\frac{dA}{dt}$ for BMF v2,

$$\frac{d}{dt}A = \mu_A\Big(\frac{K_D}{Y_* + K_D}\Big) - \gamma A - \eta_+ AI + \eta_0 C - \beta_A AU_P \tag{104}$$

where I, A synthesis rate, respectively, now depends on a new molecule Y_* with dynamics

$$\frac{d}{dt}Y_* = \mu_{Y_*} - (\gamma + \gamma_{Y_*})Y_* \tag{105}$$

such that Y_* is constitutively expressed with synthesis μ_{Y*} equal to Y synthesis rate in the steady state solution for each parameter set Θ (i.e. either $\mu_{Y*} = \mu_Y U_{ss}$), and degradation rate $\gamma_{Y*} = \gamma_Y$, before the perturbation.

S5 Using CoRa to design biomolecular feedback control mechanisms

Below, we present the details of the optimization of the CoRa function over control parameters. For this, we implemented a simple algorithm with two optimization phases: choosing for parameter values that (1) reduce the CoRa value up until $\min(\text{CoRa}) \leq \epsilon$ (with ϵ being a threshold picked by the user), and then (2) expand the range of parameter set values θ (e.g. range of μ_Y values) with $\min(\text{CoRa}) \leq \epsilon$. Multiple parameter sets might result in equivalent efficient control for a given feedback control system. This can be explored computationally by running the optimization algorithm for multiple initial conditions and/or random number chains. Iterations of the optimization process allow to determine the region of the parameter space and relationship between parameters associated to the optimal performance for the case of interest.

S5.1 Optimizing feedback control designs

The goal is to maximize the range of values of a specific parameter $\theta \in \Theta$ where $\text{CoRa}_{\theta\in\Theta}(\rho) \leq \epsilon$. For this, we consider two phases of the optimization: first minimizing the $\min(\text{CoRa}_{\theta\in\Theta}(\rho))$ up until it is less or equal ϵ; then maximizing the magnitude of $|\text{CoRa}_{\theta\in\Theta}(\rho) \leq \epsilon|$ in the explored range (in the logarithmic scale).

Error function, χ^2

Minimizing $\min(\text{CoRa}_{\theta\in\Theta}(\rho))$

We define our error function (sum of square errors) by assuming the optimal point $D = 0$, and considering the expected variance of uniform distribution $\sim U[0, 1]$ ($\sigma^2 = 0.083$). Then our error function in the initial phase of the optimization is:

$$\chi^2 = \frac{(0 - \min(\text{CoRa}_{\theta\in\Theta}(\rho)))^2}{2\sigma^2} \tag{106}$$

$$= \frac{\min(\text{CoRa}_{\theta\in\Theta}(\rho))^2}{2\sigma^2} \tag{107}$$

Maximizing $|\text{CoRa}_{\theta\in\Theta}(\rho) \leq \epsilon|$

We assume the optimal point $D = 1$ for all values of $\theta \in \Theta$ in the range of interest, then

$$\int D d\theta \quad = \quad \theta| = \theta_{max} - \theta_{min} = r \tag{108}$$

And for each data point θ_i, y_i is 1 if $\text{CoRa}_{\theta_i\in\Theta}(\rho) \leq \epsilon$, 0 otherwise. Then $(D_i - y_i)^2 = 0$ for the range where $\text{CoRa}_{\theta\in\Theta}(\rho) \leq \epsilon$, 1 otherwise. Finally,

$$\int (D_i - y_i)^2 = r - |\text{CoRa}_{\theta_i\in\Theta}(\rho) \leq \epsilon| \tag{109}$$

And the range of interest is maximized as this value is minimized. Then, our error function in this phase of the optimization is:

$$\chi^2 \quad = \quad \frac{r - |\text{CoRa}_{\theta_i\in\Theta}(\rho) \leq \epsilon|}{2\sigma^2} \tag{110}$$

We initially tried using the variance of a uniform function $\sim U[0, r]$ ($\sigma^2 = 0.083r^2$) for the error function, but it resulted in very noisy simulations. So we opted for the same variance than when minimizing $\min(\text{CoRa}_{\theta\in\Theta}(\rho))$ ($\sigma^2 = 0.083$).

Metropolis Random Walk algorithm

For each phase, an error function is defined, and a Metropolis Random Walk algorithm implemented as follows:

1. Choose some initial parameters Θ_1 and calculate the corresponding likelihood.
2. Iterate over $t = \{1, 2, ..., t_{MAX}\}$ as follows:
   (a) Draw a random proposal $\phi \sim \Theta_{(t)} \times 10^{\mathcal{N}_{||\Theta||}(0,\Sigma)}$ where $\mathcal{N}_{||\Theta||}(0, \Sigma)$ is a Multivariate Normal distribution with the same dimension as $\Theta_{(t)}$, mean zero and covariance matrix $\Sigma = 0.1$.
   (b) We construct a likelihood function using a Gaussian function:

   $$P(D|\Theta) = \exp(-\chi^2) \tag{111}$$

   where Θ is the set of parameter to be optimized, D is the optimal data, and χ^2 is the error function (which depends on the optimization phase). Note the likelihood is maximal when the error is minimal. Then we calculate the likelihood ratio:

   $$\frac{\mathcal{L}_*}{\mathcal{L}_{(t)}} = \frac{P(D|\phi)}{P(D|\Theta_{(t)})} = exp(-\chi^2_* + \chi^2_{(t)}) \tag{112}$$

   Accept the proposed ϕ if the ratio is larger than a random number $\sim U[0, 1]$. The proposed value is always accepted if the error is smaller (i.e. it's better).
   (c) Update parameters $\Theta_{(t+1)} \leftarrow \phi$ with probability $\min(1, \frac{\mathcal{L}_*}{\mathcal{L}_{(t)}})$; otherwise, $\Theta_{(t+1)} \leftarrow \Theta_{(t)}$.

References

1. R. Alves and M. A. Savageau. Extending the method of mathematically controlled comparison to include numerical comparisons. *Bioinformatics*, 16(9):786–798, sep 2000.
2. C. Briat, A. Gupta, and M. Khammash. Antithetic Integral Feedback Ensures Robust Perfect Adaptation in Noisy Biomolecular Networks. *Cell Systems*, 2(1):15–26, jan 2016.

3. T. Drengstig, X. Y. Ni, K. Thorsen, I. W. Jolma, and P. Ruoff. Robust Adaptation and Homeostasis by Autocatalysis. *The Journal of Physical Chemistry B*, 116(18):5355–5363, may 2012.

4. E. J. Hancock, J. Ang, A. Papachristodoulou, and G.-B. Stan. The Interplay between Feedback and Buffering in Cellular Homeostasis. *Cell Systems*, 5(5):498–508.e23, nov 2017.

5. A. W. Harris, J. A. Dolan, C. L. Kelly, J. Anderson, and A. Papachristodoulou. Designing Genetic Feedback Controllers. *IEEE Transactions on Biomedical Circuits and Systems*, 9(4):475–484, 2015.

6. A. H. Ng, T. H. Nguyen, M. Gómez-Schiavon, G. Dods, R. A. Langan, S. E. Boyken, J. A. Samson, L. M. Waldburger, J. E. Dueber, D. Baker, and H. El-Samad. Modular and tunable biological feedback control using a de novo protein switch. *Nature*, 572(7768):265–269, aug 2019.

7. N. Olsman, A.-A. Baetica, F. Xiao, Y. P. Leong, R. M. Murray, and J. C. Doyle. Hard Limits and Performance Tradeoffs in a Class of Antithetic Integral Feedback Networks. *Cell Systems*, 9(1):49–63.e16, jul 2019.

8. C. C. Samaniego and E. Franco. Ultrasensitive molecular controllers for quasi-integral feedback. *bioRxiv*, pages 1–27, 2018.

9. F. Xiao and J. C. Doyle. Robust Perfect Adaptation in Biomolecular Reaction Networks. *bioRxiv*, 2018.